

Gluon splitting in a shockwave

E. Iancu*, J. Laidet

Institut de Physique Théorique de Saclay, F-91191 Gif-sur-Yvette, France

Abstract

The study of azimuthal correlations in particle production at forward rapidities in proton–nucleus collisions provides direct information about high gluon density effects, like gluon saturation, in the nuclear wavefunction. In the kinematical conditions for proton–lead collisions at the LHC, the forward di–hadron production is dominated by partonic processes in which a gluon from the proton splits into a pair of gluons, while undergoing multiple scattering off the dense gluon system in the nucleus. We compute the corresponding cross–section using the Colour Glass Condensate effective theory, which enables us to include the effects of multiple scattering and gluon saturation in the leading logarithmic approximation at high energy. This opens the way towards systematic studies of angular correlations in two–gluon production, similar to previous studies for quark–gluon production in the literature. We consider in more detail two special kinematical limits: the “back–to–back correlation limit”, where the transverse momenta of the produced gluons are much larger than the nuclear saturation momentum, and the “double parton scattering limit”, where the two gluons are produced by a nearly collinear splitting occurring prior to the collision. We argue that saturation effects remain important even for relatively high transverse momenta (i.e. for nearly back–to–back configurations), leading to geometric scaling in the azimuthal distribution.

1. Introduction

At the time where this paper is about to be completed, the data acquisition for the first proton–lead run at the LHC has already been finalized and the analysis of the accumulated data is still under way. The results of this analysis should bring a wealth of information on multiparticle production in p–Pb collisions, which will complete and extend the already very interesting results obtained during the short pilot run in September 2012 [1–6].

What makes p–Pb collisions so special in the context of the LHC heavy ion program, is their capacity to measure high–density nuclear effects, while at the same time discriminating between “initial–state” and “final–state interactions”: (i) as compared to p–p collisions, they are sensitive to collective phenomena like gluon saturation and multiple scattering, which are associated with the high gluon density in the nuclear wavefunction prior to the collision (the relevant quantity in this respect is the gluon density in the transverse plane, which in a nucleus with atomic number $A \gg 1$ is larger by a factor $A^{1/3}$ as compared to a proton); (ii) as compared to Pb–Pb collisions, the nuclear effects in the initial state should not be significantly altered by “final–state interactions” — that is, by rescattering in the dense partonic medium (quark–gluon plasma) created in the intermediate stages of a nucleus–nucleus collision — and hence they should leave characteristic imprints on the particle production in the final state.

The above expectations should be taken with a grain of salt: (i) saturation effects can also manifest themselves in p–p collisions, if the center–of–mass energy is high enough and the kinematics is well chosen (e.g. in particle production at forward rapidities; see below); (ii) final–state interactions may be non–negligible even in proton–nucleus collisions, as suggested by the recent LHC data on long–range rapidity correlations (“ridge effect”) in p–Pb [3–6]. This being said, the fruitful experience with deuteron–gold collisions at RHIC [7–11] (which in that context play the same role as the p–Pb collisions at the LHC) convincingly demonstrates that, by properly choosing the observables and the kinematics, and by doing the appropriate comparisons between data for proton–proton, proton (or deuteron)–nucleus, and nucleus–nucleus collisions, one can indeed infer valuable information about both high–density effects in the initial state, and about the role of final–state interactions in nucleus–nucleus collisions.

*Corresponding author

Email addresses: edmond.iancu@cea.fr (E. Iancu), julien.laidet@cea.fr (J. Laidet)

One of the observables that have been proposed as a “smoking gun” for gluon saturation [12–16] and has already been measured at RHIC with promising results [10, 11], is the study of azimuthal correlations in the di-hadron production at forward rapidities. By “forward rapidities” we mean that, in the case of proton–nucleus (p–A) collisions, the two hadrons measured in the final state emerge in the fragmentation region of the proton (the “projectile”) and propagate at small angles w.r.t. the collision axis. This kinematics is interesting in that the measured hadrons inherit a relatively large fraction x_p of the longitudinal momentum of the projectile, but a much smaller fraction x_A of the (oppositely oriented) longitudinal momentum of the nuclear target. So, it is quite clear that the respective partonic subprocess will probe the target wavefunction at very small values $x_A \ll 1$, where the gluon density in the transverse plane is furthermore enhanced by the QCD evolution with decreasing x , or increasing energy [17–27]. Vice versa, the proton wavefunction is probed at relatively large x_p , where it is dilute. For what follows, it is useful to keep in mind that both x_p and x_A scale like the inverse of the center-of-mass energy (see Eq. (2.3) below), hence they are considerably smaller at the LHC than at RHIC (by a factor of about 25 for otherwise identical kinematical conditions).

Returning to the problem of di-hadron production, an observable which is particularly sensitive to the high density effects is the angular distribution of the produced hadrons in the transverse plane. In the absence of any nuclear effects and to leading order in perturbative QCD, the final hadrons propagate back-to-back in the transverse plane, by momentum conservation. When plotted as a function of the azimuthal angle difference $\Delta\Phi$, the respective cross-section exhibits a pronounced peak at $\Delta\Phi = \pi$, with a width reflecting higher order perturbative corrections together with the soft physics responsible for hadronization. This is correct so long as one can ignore the intrinsic transverse momenta of the participating partons from the projectile and the target (a standard assumption in the context of collinear factorization). However, in the problem at hand, the non-linear effects associated with the high gluon density in the nuclear target are expected to generate an intrinsic transverse momentum scale — the *saturation momentum* $Q_s(A, x)$ — via the phenomenon of gluon saturation. The quantity Q_s^2 is proportional to the gluon density in the transverse plane, hence it increases with the atomic number A and with $1/x$, roughly like $Q_s^2(A, x) \propto A^{1/3}/x^\lambda$ with $\lambda \simeq 0.25$. For the kinematics of interest, Q_s is expected to be of the order of a few GeV. In a p–A collision, the partons from the projectile undergo multiple scattering off the dense gluonic system in the target and thus receives transverse kicks of the order of Q_s . These random kicks will have the effect to broaden the di-hadron distribution in $\Delta\Phi$, and even wash out the back-to-back correlation between the final hadrons in the case where their transverse momenta are not much larger than Q_s . Such a broadening of the angular correlation has been indeed observed in di-hadron production at forward rapidities in d–Au collisions at RHIC [10, 11]. On the other hand, no similar effect was seen in p–p collisions, nor in particle production at *mid* rapidities in p–A collisions (at either RHIC [28] or the LHC [4]). These experimental features are in at least qualitative agreement with the predictions of saturation [15, 16].

A saturation scale $Q_s \gtrsim 2$ GeV is moderately hard, implying that saturation physics at RHIC and the LHC can be studied within perturbative QCD. The natural theoretical framework in that sense is the Colour Glass Condensate (CGC) effective theory [29–33]. This exploits the fact that the gluon modes at or near saturation have large occupation numbers, of order $1/\alpha_s$, and thus can be described as strong classical colour fields generated by ‘colour sources’ (partons) with larger values of x [34]. In this framework and to the accuracy of interest, the di-hadron production in p–A collisions is computed as the splitting of one projectile parton in the background of the strong colour field (the CGC) representing the nuclear target (see Sect. 2 below for more details). The cross-section for the partonic subprocess is then factorized as the probability for $1 \rightarrow 2$ parton splitting times gauge-invariant products of Wilson lines (one for each interacting parton) expressing the multiple scattering between the partons and the background field, in the eikonal approximation. Eventually, the products of Wilson lines must be averaged over all the possible realizations of the classical colour fields in the target. This averaging defines target correlation functions, whose calculation is the main purpose of the CGC effective theory.

The Wilson lines correlators can in principle be computed from the numerical solutions to the JIMWLK equation [22–27] — a functional renormalization group equation which governs the non-linear evolution of the nuclear gluon distribution with increasing energy, or decreasing x . Numerical solutions to JIMWLK equation are indeed feasible [35–38], but they are quite cumbersome in practice, which limits their interest for phenomenology. Fortunately, analytic approximations are also available, based on a mean field approximation to the JIMWLK equation [39–46] that has been thoroughly justified in [44, 45]. This approximation is remarkably accurate for any value of the number of colours N_c [38, 45, 46], but the corresponding calculations become considerably simpler when $N_c \gg 1$.

Previous applications of this formalism to forward di-hadron production in p–A collisions focused on

the case where the projectile parton initiating the scattering is a *quark* (q) [13, 15, 16, 47, 48]. This was indeed appropriate for d–Au collisions at RHIC, where the relevant longitudinal momentum fraction x_p is quite large: $x_p \simeq 0.1$. But the situation is different in p–Pb collisions at the LHC, where due to the larger center-of-mass energy, x_p is considerably smaller even for forward kinematics: $x_p \lesssim 10^{-2}$. For such values of x_p , the proton wavefunction is still dilute (in the sense that saturation effects are negligible and the collinear factorization applies), but the dominant partonic degrees of freedom are rather *gluons*. Motivated by this, we shall here address the corresponding process initiated by a gluon (g). This consists in the $g \rightarrow gg$ splitting¹ in the background of the target field (a “shockwave” by Lorentz contraction), followed by the hadronisation of the produced gluons. Once again, the purpose of the calculation is to express the partonic cross-section in terms of Wilson line correlators, to be eventually computed in the CGC formalism. Simplified versions of this calculation, which exploited the large- N_c approximation together with various kinematical limits [13, 14, 43], have been already presented in the literature, with results that we shall recover below.

Our final result for the cross-section for the partonic process $gA \rightarrow ggX$ is presented in Eqs. (2.4) and (2.19). This appears as the natural generalization of the corresponding result for quark splitting ($qA \rightarrow qgX$), originally obtained in [15]. Not surprisingly, the colour structure of our result is somewhat more complicated: the quark Wilson line (a colour matrix in the fundamental representation) is now replaced by a gluon Wilson line in the adjoint representation, which via the Fierz identity counts like a couple of quark Wilson lines. Accordingly, our formula (2.19) involves target correlators built with up to 8 fundamental Wilson lines (see Eqs. (2.22)–(2.24)). Yet, most of the additional complications disappear in the multicolor limit $N_c \gg 1$, where our result (2.27) contains only colour ‘dipoles’ and ‘quadrupoles’ (the 2-point and respectively 4-point functions of the fundamental Wilson lines), like the corresponding result for quark–gluon production [15]. This simplification is expected to be a generic feature of multiparticle production at high energy and large N_c [43, 49].

Thus, for large N_c at least, the ingredients of our formula (2.27) are fully explicit: the colour dipole can be computed as the solution to the Balitsky–Kovchegov equation [20, 21], and the quadrupole can be related to the dipole via the mean field approximation alluded to above [13, 43]. To obtain an explicit result also for the cross-section, one still needs to (numerically) perform the transverse integrations which appear in Eq. (2.27) — a realistic task, as demonstrated by the corresponding analysis of the $qA \rightarrow qgX$ process in Ref. [48]. Clearly, it would be very useful to perform such a detailed numerical study, in view of the LHC phenomenology. But at a qualitative level at least, the results can be easily anticipated on physical grounds, and also by analogy with the previous studies of quark–gluon production [16, 47, 48]) : the back-to-back correlation between the produced gluons should be progressively washed out when increasing the gluon rapidities (for fixed transverse momenta), or when decreasing their transverse momenta towards values of order $Q_s(A, x_A)$ (the nuclear saturation scale).

Whereas there is little doubt that saturation effects are important in the kinematical conditions just mentioned — i.e. when the transverse momenta $k_{1\perp}$ and $k_{2\perp}$ of the produced particles are comparable to the target saturation momentum Q_s —, it is perhaps less appreciated that they continue to play a role even for higher transverse momenta $k_{i\perp} \gg Q_s$ (with $i = 1, 2$). In such a case, the final particles will most likely propagate back-to-back in the transverse plane, that is, their azimuthal correlation will be strongly peaked at $\Delta\Phi = \pi$. But the width of that peak will be sensitive to the high-density nuclear effects, which control the transverse momentum imbalance between the final gluons: $|\mathbf{k}_1 + \mathbf{k}_2| \sim Q_s \ll k_{i\perp}$, with $k_{i\perp} \equiv |\mathbf{k}_i|$. Accordingly, if one is interested in the details of the azimuthal correlation, one cannot rely on the (standard) “ k_\perp -factorization” [50], which ignores the effects of multiple scattering. The proper approximation scheme to be used in this high-momentum regime (also referred to as the *back-to-back correlation limit*) has recently been clarified in Ref. [43] and applied there to several processes, including $gA \rightarrow ggX$, but only in the multicolour limit $N_c \gg 1$.

In Sect. 3.2 of this paper, we shall generalize the analysis in Ref. [43] to finite N_c , for the process at hand. We shall thus find that, in the high-momentum regime at $k_{i\perp} \gg Q_s$, the cross-section for $gA \rightarrow ggX$ can be expressed in terms of two *generalized unintegrated gluon distributions* : one built with the colour dipole, the other one with the colour quadrupole (see Eqs. (3.15)–(3.17)). The “dipole distribution”, Eq. (3.16), is well known in the literature, as it enters other processes like single inclusive gluon production [51, 52] (see Ref. [43] for more examples and references). The “quadrupole distribution” in Eq. (3.16) is to our knowledge new and specific to two-gluon production. In the single-scattering

¹A projectile gluon which scatters off the shockwave can also split into a quark–antiquark pair ($gA \rightarrow q\bar{q}X$), but the corresponding cross-section has already been computed in the literature [43]. This $q\bar{q}$ channel is suppressed at large N_c as compared to the gg channel to be discussed here and, besides, it involves a considerably simpler color structure.

approximation valid when $|\mathbf{k}_1 + \mathbf{k}_2| \gg Q_s$, these two distributions reduce to the “standard” unintegrated gluon distribution, which measures the number of gluons in the target wavefunction and enters the k_\perp -factorization. But for a typical event with $|\mathbf{k}_1 + \mathbf{k}_2| \sim Q_s$, the distributions in Eqs. (3.16)–(3.17) generalize the “standard” one by including “initial-state” and “final-state interactions”, that is, multiple scattering between the gluons involved in the splitting process $g \rightarrow gg$ and the gluon distribution in the target. As also shown in Ref. [43], via specific examples, this high-momentum ($k_\perp \gg Q_s$) limit of the CGC factorization is equivalent with the small- x limit of the TMD (“transverse-momentum dependent”) factorization — the generalization of k_\perp -factorization to a regime where the initial and/or final state interactions accompanying a hard process cannot be neglected. We therefore expect our result (3.15) to be equivalent with the respective prediction of TMD factorization. Incidentally, the fact that various partonic processes feature different versions of the (generalized) “gluon distribution” illustrates the lack of universality of the TMD factorization in this small x regime.

For more pedagogy, we shall also discuss, in Sect. 3.1, the single-scattering limit of our results and thus make contact with the standard k_\perp -factorization. This approximation, which is strictly valid when $|\mathbf{k}_1 + \mathbf{k}_2| \gg Q_s$, leads to a simple result, Eq. (3.10), that can be extrapolated for qualitative considerations towards the more interesting regime at $|\mathbf{k}_1 + \mathbf{k}_2| \sim Q_s$. This will allow us to argue that the azimuthal correlation in the high momentum regime ($k_{1\perp} \simeq k_{2\perp} \gg Q_s$) should exhibit *geometric scaling* [53–56]: the width of the angular distribution arounds its peak at $\Delta\Phi = \pi$ depends upon the kinematics of the final state only via the ratio $Q_s(A, x_A)/k_{1\perp}$.

The final kinematical limit that we shall study, known as *double parton scattering*, is the limit where the gluon branching $g \rightarrow gg$ occurs long before the scattering and is nearly collinear. In that case, the offspring gluons independently scatter off the nuclear target and thus acquire transverse momenta of the order of Q_s ($k_{1\perp} \sim k_{2\perp} \sim Q_s$), which however are *uncorrelated* with each other. Hence, the respective contribution to the cross-section is *flat* in $\Delta\Phi$: it contributes to the “pedestal” associated with the independent production of two gluons, but not to the correlation in $\Delta\Phi$. Still, this limit is interesting for the problem at hand since, as emphasized in Ref. [57], a large pedestal could obscure the physical signal of interest for us here: the disappearance of the back-to-back correlation due to multiple scattering off the nucleus. Moreover, as observed in Ref. [48] in the context of quark-gluon production, this kinematical limit introduces a logarithmic infrared divergence — actually, a *collinear* divergence — and thus requires a special treatment. The proper way to overcome this difficulty [48] and also to compute the pedestal, is to recognize that, within this limit, the process $gA \rightarrow ggX$ under consideration mixes with another partonic process, $ggA \rightarrow ggX$, in which *two* gluons from the projectile proton independently interact with the nuclear target. In particular, the collinear logarithm alluded to above is identified with one step in the DGLAP evolution [58] of the *double* gluon distribution [59], which describes the probability to find a pair of gluons inside the proton, in the collinear factorization. In practice, this amounts to computing the pedestal from the process $ggA \rightarrow ggX$, while at the same time subtracting the would-be infrared divergent contribution to the process $gA \rightarrow ggX$, to avoid double counting (see Sect. 3.3 for details).

2. Forward di-gluon production in p-A collisions from the CGC

This section will present our main calculation, that of the cross-section for inclusive two-gluon production at forward rapidities in p-A collisions. To start with, we shall briefly review the CGC formalism, that will be used for describing the nuclear wavefunction and the scattering between the partons from the projectile and the nuclear target. Then, in Sects. 2.2 and 2.3 we shall construct, first, the amplitude and then the cross-section for the partonic process $gA \rightarrow ggA$. Finally, in Sect. 2.4 we shall consider the large- N_c limit of our result and thus make contact with previous calculations in the literature.

2.1. Generalities on the CGC formalism and the cross-section

As discussed in the Introduction, for the purpose of computing forward particle production in p-A collisions, one can describe the nuclear target in the CGC effective theory [29–33]. In this formalism, the small- x gluon modes with large occupation numbers are treated as (typically strong) classical colour fields radiated by “sources” (the comparatively fast partons with $x' \gg x$) which are frozen by Lorentz time dilation in some random configuration. Then the multiple scattering between the partons from the projectile and the dense gluonic system in the target is computed — in a suitable Lorentz frame and with a suitable choice for the gauge (see below) — as the scattering off this strong colour field in the eikonal approximation. That is, each projectile parton which participates in the scattering is assumed to preserve a straight-line trajectory (meaning a fixed position in the transverse plane) and merely accumulate a phase

describing its colour rotation by the target “background” field. In a non-Abelian gauge theory like QCD, this phase is a colour matrix in the appropriate representation of the gauge group (here, $SU(N_c)$ with $N_c = 3$), known as a “Wilson line”. The partonic cross-section is obtained by summing (averaging) over the final (initial) colour indices of the partons from the projectile — a procedure which connects the various Wilson lines into gauge-invariant correlators — and by averaging over all the possible realizations of the colour fields in the target, with a functional probability distribution known as the “CGC weight function”. This last quantity, which encodes the relevant information about multi-gluon correlators in the target wavefunction in the non-linear regime at small x (i.e., in the presence of saturation), is the key ingredient of the CGC effective theory. It can be constructed via a renormalization group analysis in perturbative QCD, which consists in integrating out quantum gluon fluctuations in layers of $Y \equiv \ln(1/x)$ to “leading logarithmic accuracy” (that is, by preserving the quantum effects enhanced by a factor $\alpha_s Y$), but to all orders in the classical colour field built in the previous steps. (Once again, the background field effects are treated in the eikonal approximation.) This analysis leads to a functional Fokker-Planck equation describing the evolution of the CGC weight function with increasing Y , the JIMWLK (Jalilian-Marian, Iancu, McLerran, Weigert, Leonidov, Kovner) equation [22–27]. This functional equation is equivalent to an infinite hierarchy of non-linear evolution equations for the correlators of the Wilson lines, originally derived by Balitsky [20]. A suitable initial condition for the B-JIMWLK evolution at low energy (say, at $x_0 = 0.01$) is provided by the McLerran-Venugopalan model [34] for the gluon distribution in a large nucleus.

We now focus on the problem of interest for us here: two-gluon production in p-A collisions. We take x^3 as the collision (“longitudinal”) axis and choose the proton to be a right-mover (so that the nucleus is a left-mover). We shall systematically use light-cone coordinates², in which e.g. the proton 4-momentum reads $P^\mu = (P^+, 0, \mathbf{0})$, with $P^+ > 0$. It is convenient to work in the “projectile light-cone gauge” $A_a^+ = 0$, since with this choice the colour current $J_a^\mu = \delta^{\mu-} J_a^-$ of the target is not affected by the interaction (see e.g. the discussion in [60]). In this gauge, the target background field is particularly simple: it has only a “minus” component, $\mathcal{A}_a^\mu = \delta^{\mu-} \mathcal{A}_a^-$, which is moreover independent of x^- (the target light-cone “time”) by Lorentz time dilation, and localized near $x^+ = 0$ (a “shockwave”), by Lorentz contraction. The CGC weight function is then conveniently expressed as the probability distribution $\mathcal{W}_Y[\mathcal{A}^-]$ for this non-zero component $\mathcal{A}_a^-(x^+, \mathbf{x})$, and the target average is defined as

$$\langle \mathcal{O}[\mathcal{A}^-] \rangle_Y = \int [\mathcal{D}\mathcal{A}^-] \mathcal{W}_Y[\mathcal{A}^-] \mathcal{O}[\mathcal{A}^-], \quad (2.1)$$

for any scattering-related observable $\mathcal{O}[\mathcal{A}^-]$, such as a gauge invariant product of Wilson lines. Specifically, a gluon from the projectile with transverse coordinate \mathbf{x} will “feel” the target shockwave via the color precession $\tilde{U}_{ab}(\mathbf{x})$, where $a, b = 1, 2, \dots, N_c^2 - 1$ are colour indices for the adjoint representation and

$$\tilde{U}(\mathbf{x}) = \mathcal{P} \exp \left[ig \int dx^+ \mathcal{A}_a^-(x^+, \mathbf{x}) T^a \right], \quad (2.2)$$

is a Wilson line. (\mathcal{P} denotes path-ordering in x^+ and $(T^a)_{bc} = -if^{abc}$ are the gauge group generators in the adjoint representation.) The integral over x^+ in Eq. (2.2) formally extends along the gluon world-line, but in practice it is restricted to a narrow region near $x^+ = 0$, where lies the support of the target shockwave.

In Eq. (2.1), $Y \equiv \ln(1/x_A)$ with x_A the longitudinal momentum fraction of a typical gluon from the target which participates in the collision. To the accuracy of interest, this can be estimated by assuming a $2 \rightarrow 2$ partonic process, that is, $gg \rightarrow gg$. For definiteness, we shall specify the kinematics in the center-of-mass frame for the proton-nucleon³ collision. (This Lorentz frame is similar to, but not exactly the same as, the laboratory frame for p-Pb collisions at the LHC.) Using energy-momentum conservation, one can easily relate the longitudinal momentum fractions x_p and x_A of the two gluons (from the proton

²For a generic 4-vector X^μ with ordinary coordinates $X^\mu = (X^0, X^1, X^2, X^3)$, where X^3 refers to the longitudinal direction and X^i , $i = 1, 2$, to the transverse ones, the corresponding light-cone coordinates are defined as $X^\mu = (X^+, X^-, \mathbf{X})$ with $X^\pm = (X^0 \pm X^3)/\sqrt{2}$ and $\mathbf{X} = (X^1, X^2)$. We refer to \mathbf{X} as the “transverse component” and denote its modulus as $X_\perp = |\mathbf{X}|$.

³The “nucleon” is the particular proton or neutron from the target which is involved in the collision. Notice that the momentum fraction x_A is defined w.r.t. the longitudinal momentum Q^- of that particular nucleon ($x_A = q^-/Q^-$, with q^- the longitudinal momentum of the participating gluon), and not w.r.t. the nucleus as a whole. In the COM frame under consideration, one has $P^+ = Q^- = \sqrt{s}/2$.

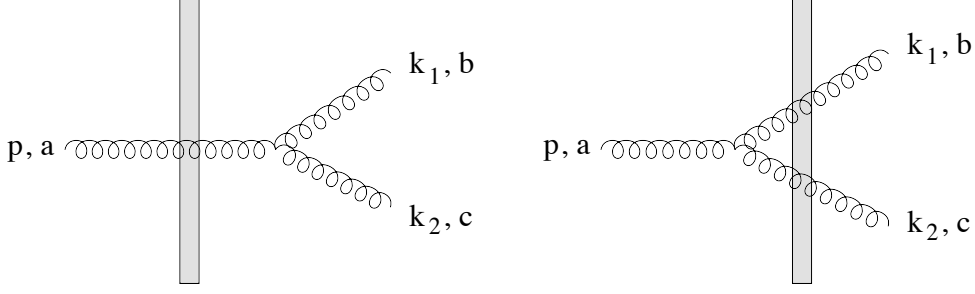


Figure 1: Feynman graphs for the gluon splitting in the background of the shockwave.

and the nucleus, respectively) which initiate the scattering to the kinematics of the final state. One finds

$$x_p = \frac{k_{1\perp}}{\sqrt{s}} e^{y_1} + \frac{k_{2\perp}}{\sqrt{s}} e^{y_2}, \quad x_A = \frac{k_{1\perp}}{\sqrt{s}} e^{-y_1} + \frac{k_{2\perp}}{\sqrt{s}} e^{-y_2}, \quad (2.3)$$

where \sqrt{s} is energy per nucleon pair in the COM frame, $y_i \equiv -\ln \tan(\theta_i/2)$ with $i = 1, 2$ are the pseudo-rapidities of the two produced gluons and $k_{i\perp}$ are the respective transverse momenta. For “forward rapidities”, that is, when y_1 and y_2 are both positive and quite large, x_A is much smaller than x_p , as anticipated in the Introduction. E.g., for “semi-hard” $k_{i\perp} \sim 2$ GeV and for $y_i \simeq 4$, one finds that in p-Pb collisions at the LHC ($\sqrt{s} = 5.02$ TeV), one has $x_p \simeq 0.02$ and $x_A \simeq 5 \times 10^{-5}$. For such values of x_p , the proton wavefunction is dominated by gluons (see e.g. [61]), but their density is still quite low, so the collinear factorization applies on the projectile side. On the other hand, on the target side, our experience with RHIC [62] suggests that saturation effects should be indeed important for such a small x_A and a large Pb nucleus, so the nuclear wavefunction should be treated as a CGC. That is, the relevant partonic process should better be viewed as a gluon-shockwave scattering ($gA \rightarrow ggX$). In that case, the final gluons propagating at forward rapidities are produced via the dissociation of the participating gluon from the projectile, a process which can occur either after, or before, the scattering off the shockwave, as illustrated in Fig. 1. The partonic amplitude involves one adjoint Wilson line in the first case and two such lines in the second case, hence the corresponding cross-section (obtained by taking the modulus squared) contains up to four gluonic Wilson lines. This will be computed in the remaining part of this section, by using Feynman rules to be described in Appendix A.2.

To conclude this general discussion, let us exhibit the formula relating the partonic cross-section to the amplitude squared that we shall later compute. In the spirit of the collinear factorization, both the initial gluon with 4-momentum p^μ and the emerging ones, with 4-momenta k_i^μ ($i = 1, 2$), will be put on-shell; in particular $p^\mu = (p^+, 0, \mathbf{0})$, with $p^+ = x_p P^+$. Due to the homogeneity of the target field in x^- , the “plus” component of the momentum will be preserved by the scattering: $p^+ = k_1^+ + k_2^+$. The transverse momenta however are not conserved, since the target can transfer a typical momentum $Q_s(A, x_A)$. Accordingly, the cross-section for the partonic process $gA \rightarrow ggX$ has the general structure (see e.g. [63] for a derivation of this formula in a similar context)

$$\frac{d\sigma(gA \rightarrow ggX)}{dy_1 dy_2 d^2\mathbf{k}_1 d^2\mathbf{k}_2} = \frac{1}{8(2\pi)^6 p^+} \langle |\mathcal{M}(g(p)A \rightarrow g(k_1)g(k_2))|^2 \rangle_Y 2\pi \delta(p^+ - k_1^+ - k_2^+). \quad (2.4)$$

where $\mathcal{M}(g(p)A \rightarrow g(k_1)g(k_2))$ denotes the corresponding amplitude, with the colour and polarization indices omitted, for convenience (see Eq. (2.6) below for more details). Furthermore, the notation $\langle \dots \rangle_Y$ includes the average (sum) over the initial (final) colour and polarization states of the three participating gluons and the CGC average over the background field evaluated at $Y = \ln(1/x_A)$. The final gluons carry transverse momenta $\mathbf{k}_1, \mathbf{k}_2$ and rapidities y_1, y_2 , with $y_i = \frac{1}{2} \ln(k_i^+/k_i^-)$ and $k_i^- = k_{i\perp}^2/2k_i^+$.

From Eq. (2.4), one easily obtains the respective p-A cross-section ($pA \rightarrow ggX$) by convoluting with $x_p G(x_p, \mu^2)$ (the gluon distribution inside the proton) :

$$\begin{aligned} \frac{d\sigma(pA \rightarrow ggX)}{dy_1 dy_2 d^2\mathbf{k}_1 d^2\mathbf{k}_2} &= \int dx_p G(x_p, \mu^2) \frac{d\sigma(gA \rightarrow ggX)}{dy_1 dy_2 d^2\mathbf{k}_1 d^2\mathbf{k}_2} \\ &= \frac{1}{256\pi^5 (p^+)^2} x_p G(x_p, \mu^2) \langle |\mathcal{M}(g(p)A \rightarrow g(k_1)g(k_2))|^2 \rangle_Y. \end{aligned} \quad (2.5)$$

To the accuracy of interest, the factorization scale μ^2 should be chosen of the order of a typical value of the final transverse momenta. The *physical* cross-section, which refers to a hadronic final state ($pA \rightarrow hhX$), can finally be obtained by convoluting Eq. (2.5) with the fragmentation functions for gluons evolving into hadrons.

2.2. The amplitude

As already mentioned, the partonic process $gA \rightarrow ggX$ involves the two diagrams illustrated in Fig. 1. Using the Feynman rules detailed in Appendix A.2, it is straightforward to write down the corresponding contributions to the scattering amplitude :

$$\begin{aligned}
i\mathcal{M}(g(p, a)A \rightarrow g(k_1, b)g(k_2, c)) = & -gf^{dbc}\epsilon_\mu(p)\epsilon^{\nu*}(k_1)\epsilon^{\rho*}(k_2)\Gamma_{\sigma\nu\rho}(k_1 + k_2, k_1, k_2) \\
& \times 2p^+\beta^{\mu i}(\mathbf{p}, p^+) \frac{i\beta^{\sigma i}(\mathbf{k}_1 + \mathbf{k}_2, p^+)}{(k_1 + k_2)^2 + i\epsilon} \int d^2\mathbf{x} \tilde{U}_{da}(\mathbf{x}) e^{-i\mathbf{x}\cdot(\mathbf{k}_1 + \mathbf{k}_2 - \mathbf{p})} \\
& + gf^{aef}\epsilon^\mu(p)\epsilon_\nu^*(k_1)\epsilon_\rho^*(k_2) \int_{l^+=k^+} \frac{dl^- d^2\mathbf{l}}{(2\pi)^3} \Gamma_{\mu\sigma\lambda}(p, l, p-l) \\
& \times 2k_1^+\beta^{\nu i}(\mathbf{k}_1, k_1^+) \frac{i\beta^{\sigma i}(\mathbf{l}, k_1^+)}{l^2 + i\epsilon} \int d^2\mathbf{x} \tilde{U}_{be}(\mathbf{x}) e^{-i\mathbf{x}\cdot(\mathbf{k}_1 - \mathbf{l})} \\
& \times 2k_2^+\beta^{\rho j}(\mathbf{k}_2, k_2^+) \frac{i\beta^{\lambda j}(\mathbf{p} - \mathbf{l}, k_2^+)}{(p-l)^2 + i\epsilon} \int d^2\mathbf{y} \tilde{U}_{cf}(\mathbf{y}) e^{-i\mathbf{y}\cdot(\mathbf{k}_2 - \mathbf{p} + \mathbf{l})}.
\end{aligned} \tag{2.6}$$

We employ the convention that repeated indices are summed over. The transverse momentum \mathbf{p} of the initial gluon is momentarily kept generic, for more clarity, but it will be eventually set to zero. All the external momenta, p , k_1 and k_2 , are on their mass-shell.

The polarization indices have not been explicitly written in Eq. (2.6), to alleviate notations. The gauge condition $A^+ = 0$ together with the Ward identity $k \cdot \epsilon(k) = 0$ imply the constraints $\epsilon^+ = 0$ and $\epsilon^-(k) = k^i \epsilon^i(k)/k^+$. $\Gamma_{\mu\nu\rho}(k, p, q)$ denotes the three-gluon vertex with the colour factor omitted: the momentum k is incoming, while p and q are outgoing (see Eq. (A.15) for the explicit expression). The symbol $\beta^{\mu i}(\mathbf{p}, k^+)$ may be viewed as the ‘square-root’ of the tensorial structure of the gluon propagator in the background field. As discussed in detail in Appendix A.2, this propagator is conveniently written as (in momentum space; see Eq. (A.11))

$$G_{ab}^{\mu\nu}(k^-, \mathbf{k}; q^-, \mathbf{q}; k^+) = \beta^{\mu i}(\mathbf{k}, k^+) \beta^{\nu i}(\mathbf{q}, k^+) G_{ab}(k^-, \mathbf{k}; q^-, \mathbf{q}; k^+) \tag{2.7}$$

where $G_{ab}(k^-, \mathbf{k}; q^-, \mathbf{q}; k^+)$ is the respective scalar propagator and

$$\beta^{\mu i}(\mathbf{q}, k^+) = \delta^{\mu-} \frac{q^i}{k^+} + \delta^{\mu i}. \tag{2.8}$$

As a guidance to see how Eq. (2.6) has been derived, let us consider the second process in Fig. 1, i.e. splitting before the scattering. Using Eq. (A.21), the upper final leg attached to the shockwave combined with the propagator running from the branching vertex to the shockwave contributes as

$$-2k_1^+ \epsilon_\nu^*(k_1) \beta^{\nu i}(\mathbf{k}_1, k_1^+) \frac{i\beta^{\sigma i}(\mathbf{l}, k_1^+)}{l^2 + i\epsilon} \int d^2\mathbf{x} \tilde{U}_{be}(\mathbf{x}) e^{-i\mathbf{x}\cdot(\mathbf{k}_1 - \mathbf{l})}. \tag{2.9}$$

l is the momentum running between the vertex and the shockwave through the upper branch. Since the plus component of the momentum remains unaffected by the shockwave, this fixes $l^+ = k_1^+$. However, the other components are not fixed and one has to integrate the whole diagram over l^- and \mathbf{l} . There is a similar expression for the lower final leg but the final momentum is k_2 and the momentum flowing between the vertex and the shockwave is $p-l$, with $(p-l)^+ = k_2^+$. Finally, the vertex brings a factor $gf^{aef}\Gamma_{\mu\sigma\lambda}(p, l, p-l)$ and the initial gluon introduces the polarization vector $\epsilon^\mu(p)$. The first diagram in Fig. 1 is computed in a similar way.

In Eq. (2.6), the integral over l^- is performed using the residue theorem. The result is to set l on-shell (i.e. $l^- = \mathbf{l}^2/2k_1^+$) and to replace $i/l^2 \rightarrow 2\pi/2k_1^+$. (The $i\epsilon$ prescriptions play no role since none of the denominators is vanishing.) We introduce the splitting fraction z such that $k_1^+ = zp^+$ and $k_2^+ = (1-z)p^+$. This is related to the kinematics of the produced gluons via

$$z = \frac{k_{1\perp} e^{y_1}}{k_{1\perp} e^{y_1} + k_{2\perp} e^{y_2}}. \tag{2.10}$$

Then the denominators in Eq. (2.6) can be rewritten as :

$$\begin{aligned}(k_1 + k_2)^2 &= \frac{1}{z(1-z)}((1-z)\mathbf{k}_1 - z\mathbf{k}_2)^2 \\ (p-l)^2 &= -\frac{1}{z}\mathbf{l}^2.\end{aligned}\tag{2.11}$$

At this point, we use Eq. (A.14) to replace the polarization 4-vectors by their transverse components alone. After these manipulations, the amplitude (2.6) becomes

$$\begin{aligned}i\mathcal{M}(g(p, a)A \rightarrow g(k_1, b)g(k_2, c)) &= g\epsilon^i(p)\epsilon^{j*}(k_1)\epsilon^{k*}(k_2) \times \\ &\times \left[f^{dbc} \frac{2ip^+z(1-z)}{((1-z)\mathbf{k}_1 - z\mathbf{k}_2)^2} \beta^{\mu i}(\mathbf{k}_1 + \mathbf{k}_2, p^+) \beta^{\nu j}(\mathbf{k}_1, k_1^+) \beta^{\rho k}(\mathbf{k}_2, k_2^+) \Gamma_{\mu\nu\rho}(k_1 + k_2, k_1, k_2) \right. \\ &\quad \times \int d^2\mathbf{x} \tilde{U}_{da}(\mathbf{x}) e^{-i\mathbf{x} \cdot (\mathbf{k}_1 + \mathbf{k}_2 - \mathbf{p})} \\ &\quad - f^{aef} \int \frac{d^2\mathbf{l}}{(2\pi)^2} \frac{2ik_2^+z}{\mathbf{l}^2} \beta^{\mu i}(\mathbf{p}, p^+) \beta^{\nu j}(\mathbf{l}, k_1^+) \beta^{\rho k}(\mathbf{p} - \mathbf{l}, k_2^+) \Gamma_{\mu\nu\rho}(p, l, p-l) \\ &\quad \left. \times \int d^2\mathbf{x} d^2\mathbf{y} \tilde{U}_{be}(\mathbf{x}) \tilde{U}_{cf}(\mathbf{y}) e^{-i\mathbf{x} \cdot (\mathbf{k}_1 - \mathbf{l}) - i\mathbf{y} \cdot (\mathbf{k}_2 - \mathbf{p} + \mathbf{l})} \right].\end{aligned}\tag{2.12}$$

2.3. The splitting probability

Given the above expression, Eq. (2.12), for the splitting amplitude in the presence of the shockwave, we shall now compute the associated probability, by taking the modulus squared of the amplitude, summing over the colour and polarization states of the two final gluons, averaging over the corresponding states of the initial gluon, and, finally, averaging over the random background field, with the help of the CGC weight function. This procedure is summarized in

$$\langle |\mathcal{M}(g(p)A \rightarrow g(k_1)g(k_2))|^2 \rangle_Y \equiv \frac{1}{2(N_c^2 - 1)} \sum_{pol.} \sum_{abc} \left\langle |\mathcal{M}(g(p, a)A \rightarrow g(k_1, b)g(k_2, c))|^2 \right\rangle_Y,$$

with the CGC average as defined in Eq. (2.1). For more clarity, the calculation of the r.h.s. of Eq. (2.13) will be split into two stages : first, we shall take care of the Lorentz structure, by performing the sum and average over polarizations, then the sum and average over colours (including the CGC average).

After taking the modulus squared of the amplitude in (2.12), the sum over polarizations is readily performed by using

$$\sum_{pol.} \epsilon^i(k) \epsilon^{j*}(k) = \delta^{ij}.\tag{2.13}$$

Notice that the r.h.s. of the above equation is independent of the momentum k carried by the polarization vector. Hence, an expression like $\epsilon^i(p) \beta^{\mu i}(\mathbf{k}, k^+)$, after being squared and summed over polarizations, will give a result which depends only upon k , and not also upon p .

The computation of the modulus squared of the vertex functions which appear in Eq. (2.12) — this leads to terms of the form $\sum_{ijk} |\beta^{i\mu} \beta^{j\nu} \beta^{k\rho} \Gamma_{\mu\nu\rho}|^2$ — is quite lengthy but straightforward, and it is deferred to Appendix B.1. Using the respective results, as shown in Eq. (B.1), one eventually obtains (as compared to Eq. (2.12), we shall from now on set $\mathbf{p} = 0$)

$$\begin{aligned}|\mathcal{M}(g(p)A \rightarrow g(k_1)g(k_2))|^2 &= \frac{16g^2(p^+)^2 z(1-z)}{N_c^2 - 1} P_{g \leftarrow g}(z) \times \\ &\times \sum_{abc} \left| f^{dbc} \frac{(1-z)k_1^i - zk_2^i}{((1-z)\mathbf{k}_1 - z\mathbf{k}_2)^2} \int d^2\mathbf{x} \tilde{U}_{da}(\mathbf{x}) e^{-i\mathbf{x} \cdot (\mathbf{k}_1 + \mathbf{k}_2)} - \right. \\ &\quad \left. - f^{aef} \int \frac{d^2\mathbf{l}}{(2\pi)^2} \frac{l^i}{\mathbf{l}^2} \int d^2\mathbf{x} d^2\mathbf{y} \tilde{U}_{be}(\mathbf{x}) \tilde{U}_{cf}(\mathbf{y}) e^{-i\mathbf{x} \cdot (\mathbf{k}_1 - \mathbf{l}) - i\mathbf{y} \cdot (\mathbf{k}_2 + \mathbf{l})} \right|^2,\end{aligned}\tag{2.14}$$

where $P_{g \leftarrow g}(z)$ is the DGLAP gluon-to-gluon splitting function :

$$P_{g \leftarrow g}(z) \equiv \frac{z}{1-z} + \frac{1-z}{z} + z(1-z).\tag{2.15}$$

This result can be rewritten in a more suggestive form by using the following identities,

$$\begin{aligned} \int \frac{d^2 \mathbf{l}}{(2\pi)^2} \frac{l^i}{l^2} e^{i\mathbf{l} \cdot (\mathbf{x} - \mathbf{y})} &= \frac{i}{2\pi} \frac{x^i - y^i}{(\mathbf{x} - \mathbf{y})^2} \\ \frac{(1-z)k_1^i - zk_2^i}{((1-z)\mathbf{k}_1 - z\mathbf{k}_2)^2} &= \frac{i}{2\pi} \int d^2 \mathbf{y} \frac{x^i - y^i}{(\mathbf{x} - \mathbf{y})^2} e^{-i((1-z)\mathbf{k}_1 - z\mathbf{k}_2) \cdot (\mathbf{x} - \mathbf{y})}, \end{aligned} \quad (2.16)$$

in which one recognizes the derivative $\partial_x^i \Delta(\mathbf{x} - \mathbf{y})$ of the two-dimensional Coulomb propagator in the transverse plane, $\Delta(\mathbf{x}) = (1/4\pi) \ln(1/\mathbf{x}^2)$. In the present context, this plays the role of the transverse splitting function, as we shall shortly discuss. After using Eq. (2.16) and performing some changes in the integration variables, one can recast Eq. (2.14) into the form

$$\begin{aligned} |\mathcal{M}(g(p)A \rightarrow g(k_1)g(k_2))|^2 &= \frac{4g^2(p^+)^2 z(1-z)}{\pi^2(N_c^2 - 1)} P_{g \leftarrow g}(z) \\ &\sum_{abc} \left| \int d^2 \mathbf{x} d^2 \mathbf{y} \frac{x^i - y^i}{(\mathbf{x} - \mathbf{y})^2} e^{-i\mathbf{k}_1 \cdot \mathbf{x} - i\mathbf{k}_2 \cdot \mathbf{y}} \left[f^{dbc} \tilde{U}_{da}(\mathbf{b}) - f^{aef} \tilde{U}_{be}(\mathbf{x}) \tilde{U}_{cf}(\mathbf{y}) \right] \right|^2, \end{aligned} \quad (2.17)$$

which admits a transparent physical interpretation: \mathbf{x} and \mathbf{y} are the transverse coordinates of the two final gluons, whereas $\mathbf{b} \equiv z\mathbf{x} + (1-z)\mathbf{y}$, which is recognized as their center-of-mass in the transverse plane, is the respective coordinate of the original gluon. The function

$$\frac{x^i - y^i}{(\mathbf{x} - \mathbf{y})^2} = (1-z) \frac{x^i - b^i}{(\mathbf{x} - \mathbf{b})^2} = -z \frac{y^i - b^i}{(\mathbf{y} - \mathbf{b})^2} \quad (2.18)$$

is proportional to the amplitude for splitting a gluon at \mathbf{x} (or at \mathbf{y}) from an original gluon at \mathbf{b} . The first terms within the square brackets in Eq. (2.17) corresponds to the process where the original gluon interacts with the shockwave prior to splitting (left diagram in Fig. 1). The second terms describes the other situation, where the splitting occurs before the interaction and then the offspring gluons scatter off the shockwave (right diagram in Fig. 1).

It is now straightforward to explicitly compute the modulus squared in Eq. (2.17) and then perform the sum and average over the gluon colour indices. This yields

$$\begin{aligned} \langle |\mathcal{M}(g(p)A \rightarrow g(k_1)g(k_2))|^2 \rangle_Y &= \frac{4g^2 N_c}{\pi^2} (p^+)^2 z(1-z) P_{g \leftarrow g}(z) \\ &\times \int d^2 \mathbf{x} d^2 \mathbf{y} d^2 \bar{\mathbf{x}} d^2 \bar{\mathbf{y}} \frac{(\mathbf{x} - \mathbf{y}) \cdot (\bar{\mathbf{x}} - \bar{\mathbf{y}})}{(\mathbf{x} - \mathbf{y})^2 (\bar{\mathbf{x}} - \bar{\mathbf{y}})^2} e^{-i\mathbf{k}_1 \cdot (\mathbf{x} - \bar{\mathbf{x}}) - i\mathbf{k}_2 \cdot (\mathbf{y} - \bar{\mathbf{y}})} \\ &\times \left\langle \tilde{S}^{(2)}(\mathbf{b}, \bar{\mathbf{b}}) - \tilde{S}^{(3)}(\mathbf{b}, \bar{\mathbf{x}}, \bar{\mathbf{y}}) - \tilde{S}^{(3)}(\bar{\mathbf{b}}, \mathbf{x}, \mathbf{y}) + \tilde{S}^{(4)}(\mathbf{x}, \mathbf{y}, \bar{\mathbf{x}}, \bar{\mathbf{y}}) \right\rangle_Y, \end{aligned} \quad (2.19)$$

where the brackets in the last line denote the average over the background field, in the sense of Eq. (2.1) and the other notations will be shortly explained. Eq. (2.19) is our main new result in this paper: the probability for gluon splitting triggered by its interactions with the nucleus. The corresponding partonic cross-section can now be computed by inserting this result into Eq. (2.5).

Let us now explain the new notations introduced in Eq. (2.19). We have $\mathbf{b} \equiv z\mathbf{x} + (1-z)\mathbf{y}$ and $\bar{\mathbf{b}} \equiv z\bar{\mathbf{x}} + (1-z)\bar{\mathbf{y}}$, where \mathbf{x} and $\bar{\mathbf{x}}$ are the transverse coordinates of the produced gluon with momentum \mathbf{k}_1 in the direct and respectively the complex conjugate amplitude, whereas \mathbf{y} and $\bar{\mathbf{y}}$ similarly refer to the second produced gluon. Furthermore, we have denoted

$$\begin{aligned} \tilde{S}^{(2)}(\mathbf{b}, \bar{\mathbf{b}}) &= \frac{1}{N_c(N_c^2 - 1)} f^{dbc} f^{d'bc} \tilde{U}_{da}(\mathbf{b}) \tilde{U}_{d'a}(\bar{\mathbf{b}}) = \frac{1}{N_c^2 - 1} \text{Tr}[\tilde{U}(\mathbf{b}) \tilde{U}^\dagger(\bar{\mathbf{b}})] \\ \tilde{S}^{(3)}(\mathbf{b}, \bar{\mathbf{x}}, \bar{\mathbf{y}}) &= \frac{1}{N_c(N_c^2 - 1)} f^{dbc} f^{aef} \tilde{U}_{da}(\mathbf{b}) \tilde{U}_{be}(\bar{\mathbf{x}}) \tilde{U}_{cf}(\bar{\mathbf{y}}) \\ \tilde{S}^{(4)}(\mathbf{x}, \mathbf{y}, \bar{\mathbf{x}}, \bar{\mathbf{y}}) &= \frac{1}{N_c(N_c^2 - 1)} f^{aef} f^{a'e'f'} \tilde{U}_{be}(\mathbf{x}) \tilde{U}_{cf}(\mathbf{y}) \tilde{U}_{be'}(\bar{\mathbf{x}}) \tilde{U}_{cf'}(\bar{\mathbf{y}}). \end{aligned} \quad (2.20)$$

The normalization factors in Eq. (2.20) are chosen in such a way that the various functions $\tilde{S}^{(k)}$, with $k = 2, 3, 4$, approach unity in limit of a vanishing background field. Using the identity $f^{aef} \tilde{U}_{be} \tilde{U}_{cf} = \tilde{U}_{da} f^{dbc}$, it is easy to check that they can be all obtained from $\tilde{S}^{(4)}$:

$$\tilde{S}^{(2)}(\mathbf{b}, \bar{\mathbf{b}}) = \tilde{S}^{(4)}(\mathbf{b}, \mathbf{b}, \bar{\mathbf{b}}, \bar{\mathbf{b}}), \quad \tilde{S}^{(3)}(\mathbf{b}, \bar{\mathbf{x}}, \bar{\mathbf{y}}) = \tilde{S}^{(4)}(\mathbf{b}, \mathbf{b}, \bar{\mathbf{x}}, \bar{\mathbf{y}}). \quad (2.21)$$

Physically, the functions $\tilde{S}^{(k)}$ represent S -matrices for the eikonal scattering between a system of k gluons in an overall colour singlet state and the background field. For instance, $\tilde{S}^{(2)}$ corresponds to a gluonic dipole made with the original gluon in the amplitude times its hermitian conjugate in the complex conjugate amplitude. Its contribution to Eq. (2.19) represents the probability for the process in which the splitting occurs after the scattering. Similarly, $\tilde{S}^{(4)}$ (a gluonic quadrupole) describes the process where the splitting occurs prior to the scattering, and the two pieces involving $\tilde{S}^{(3)}$ describe the interference between the two possible time orderings. The identities (2.21) have a simple physical interpretation: if the two gluons produced by the splitting are very close to each other, such that one can approximate $\mathbf{x} \simeq \mathbf{y} \simeq \mathbf{b}$, then this system of two overlapping gluons scatters off the shockwave in the same way as would do their parent gluon (prior to splitting).

Not surprisingly, the general structure of the probability for gluon splitting in Eq. (2.19) is very similar to that for the corresponding quark splitting ($qA \rightarrow qgX$), as computed in [15]. The main difference refers, as expected, to the replacement of the quark Wilson lines (in the fundamental representation of the colour group) by adjoint Wilson lines for gluons. Moreover, Eq. (2.19) generalizes previous results for the gluon splitting [13, 14, 43] obtained in special kinematical limits and for large N_c . We shall later recover these previous results by taking the appropriate limits in Eq. (2.19).

2.4. The limit of a large number of colours

The expression (2.19) for two-gluon production is still formal: in order to transform this expression into an explicit function of the kinematic variables $\mathbf{k}_1, \mathbf{k}_2, Y$ and z of the final state, one still needs to compute the CGC expectation values of the multipole operators introduced in Eq. (2.20) and then perform the various Fourier transforms appearing in Eq. (2.19). It would be very interesting to complete this program (in particular, in view of applications to phenomenology), but this goes beyond our purposes in this paper. Rather, we shall merely indicate the steps allowing to simplify the calculation and make it tractable in the limit where the number of colours N_c is large.

In view of taking the large N_c limit, it is convenient to express the gluonic multipole operators in Eq. (2.20) in terms of *quark* operators, i.e. of Wilson lines in the fundamental representation. This can be done by using the group identities listed in Eq. (B.2), namely $\tilde{U}_{ab}^\dagger = 2\text{tr}(t^a U^\dagger t^b U)$ together with the Fierz identity. (The t^a 's are the gauge group generators in the fundamental representation and U is the respective Wilson line, obtained by replacing $T^a \rightarrow t^a$ in Eq. (2.2).) After straightforward manipulations, the function $\tilde{S}^{(4)}$ is eventually rewritten as follows

$$\begin{aligned} \tilde{S}^{(4)}(\mathbf{x}, \mathbf{y}, \mathbf{u}, \mathbf{v}) = & \frac{N_c^2}{2(N_c^2 - 1)} \left[Q(\mathbf{x}, \mathbf{y}, \mathbf{v}, \mathbf{u}) S(\mathbf{u}, \mathbf{x}) S(\mathbf{y}, \mathbf{v}) + Q(\mathbf{y}, \mathbf{x}, \mathbf{u}, \mathbf{v}) S(\mathbf{x}, \mathbf{u}) S(\mathbf{v}, \mathbf{y}) \right. \\ & \left. - \frac{1}{N_c^2} O(\mathbf{v}, \mathbf{x}, \mathbf{u}, \mathbf{v}, \mathbf{y}, \mathbf{u}, \mathbf{x}, \mathbf{y}) - \frac{1}{N_c^2} O(\mathbf{v}, \mathbf{u}, \mathbf{x}, \mathbf{v}, \mathbf{y}, \mathbf{x}, \mathbf{u}, \mathbf{y}) \right], \end{aligned} \quad (2.22)$$

where the various terms in the r.h.s. are multipoles (i.e. single-trace operators) built with Wilson lines in the fundamental representation. Namely, we shall need the respective dipole, quadrupole, hexapole, and octupole, defined as

$$\begin{aligned} S(\mathbf{x}, \mathbf{y}) &= \frac{1}{N_c} \text{tr} [U(\mathbf{x}) U^\dagger(\mathbf{y})] \\ Q(\mathbf{x}, \mathbf{y}, \mathbf{u}, \mathbf{v}) &= \frac{1}{N_c} \text{tr} [U(\mathbf{x}) U^\dagger(\mathbf{y}) U(\mathbf{u}) U^\dagger(\mathbf{v})] \\ H(\mathbf{x}, \mathbf{y}, \mathbf{u}, \mathbf{v}, \mathbf{w}, \mathbf{z}) &= \frac{1}{N_c} \text{tr} [U(\mathbf{x}) U^\dagger(\mathbf{y}) U(\mathbf{u}) U^\dagger(\mathbf{v}) U(\mathbf{w}) U^\dagger(\mathbf{z})] \\ O(\mathbf{x}, \mathbf{y}, \mathbf{u}, \mathbf{v}, \mathbf{w}, \mathbf{z}, \mathbf{t}, \mathbf{s}) &= \frac{1}{N_c} \text{tr} [U(\mathbf{x}) U^\dagger(\mathbf{y}) U(\mathbf{u}) U^\dagger(\mathbf{v}) U(\mathbf{w}) U^\dagger(\mathbf{z}) U(\mathbf{t}) U^\dagger(\mathbf{s})]. \end{aligned} \quad (2.23)$$

These are formally the operators which describe the scattering between a quark-antiquark ($q\bar{q}$) colour dipole, a $q\bar{q}q\bar{q}$ colour quadrupole, etc, off the background field. The corresponding expressions for $\tilde{S}^{(2)}$ and $\tilde{S}^{(3)}$ follow from (2.21) :

$$\begin{aligned} \tilde{S}^{(2)}(\mathbf{x}, \mathbf{u}) &= \frac{N_c^2}{N_c^2 - 1} \left[S(\mathbf{x}, \mathbf{u}) S(\mathbf{u}, \mathbf{x}) - \frac{1}{N_c^2} \right] \\ \tilde{S}^{(3)}(\mathbf{x}, \mathbf{u}, \mathbf{v}) &= \frac{N_c^2}{2(N_c^2 - 1)} [S(\mathbf{v}, \mathbf{u}) S(\mathbf{u}, \mathbf{x}) S(\mathbf{x}, \mathbf{v}) + S(\mathbf{u}, \mathbf{v}) S(\mathbf{x}, \mathbf{u}) S(\mathbf{v}, \mathbf{x}) - \\ & \quad - \frac{1}{N_c^2} H(\mathbf{v}, \mathbf{x}, \mathbf{u}, \mathbf{v}, \mathbf{x}, \mathbf{u}) - \frac{1}{N_c^2} H(\mathbf{v}, \mathbf{u}, \mathbf{x}, \mathbf{v}, \mathbf{u}, \mathbf{x})]. \end{aligned} \quad (2.24)$$

We are now in a position to explain the simplifications occurring in the limit where $N_c \gg 1$. They are mainly of three types: type (i) refers to the structure of the scattering operators, type (ii) to their target expectation values (the Wilson line correlators), and type (iii) to the structure of the B-JIMWLK evolution equations obeyed by these correlators.

(i) Within Eqs. (2.22) and (2.24), all the multipole operators higher than the quadrupole are accompanied by an explicit factor of $1/N_c^2$ and hence they are suppressed⁴ as $N_c \rightarrow \infty$. This reduction of the multipole functional space to dipoles and quadrupoles, occurring at large N_c , has been recently argued [49] to be a general property, which holds for any production process of the dilute-dense type (at least, within the limits of the CGC formalism).

(ii) Averages of products of multipoles factorize into products of averages of individual multipoles. (This is a generic property of multi-trace expectation values.) For instance, the gluonic dipole S -matrix shown in the first line of Eq. (2.24) can be approximated as

$$\langle \tilde{S}^{(2)}(\mathbf{x}, \mathbf{u}) \rangle_Y = \langle S(\mathbf{u}, \mathbf{x}) \rangle_Y \langle S(\mathbf{x}, \mathbf{u}) \rangle_Y \quad (N_c \rightarrow \infty). \quad (2.25)$$

In general, the dipole expectation value is *not* symmetric: whenever non-vanishing, the difference $\langle S(\mathbf{u}, \mathbf{x}) - S(\mathbf{x}, \mathbf{u}) \rangle_Y$ is purely imaginary and C -odd and describes the amplitude for odderon exchanges in the dipole-target scattering [64, 65]. However, if the initial condition for the dipole amplitude at low energy is real, as is e.g. the case within the MV model [34], then this property will be preserved by the JIMWLK evolution up to arbitrarily high energy. A similar applies to the quadrupole: if this is real at $Y = Y_0$ (as is indeed the case within the MV model), then it remains real for any $Y > Y_0$ and, moreover, the following symmetry property holds: $\langle Q(\mathbf{x}, \mathbf{y}, \mathbf{v}, \mathbf{u}) \rangle_Y = \langle Q(\mathbf{y}, \mathbf{x}, \mathbf{u}, \mathbf{v}) \rangle_Y$ (cf. Eq. (2.22)).

Accordingly, at large N_c and for initial conditions provided by the MV model, the Wilson line correlators relevant for two-gluon production simplify to

$$\begin{aligned} \langle \tilde{S}^{(2)}(\mathbf{x}, \mathbf{u}) \rangle_Y &\simeq \langle S(\mathbf{u}, \mathbf{x}) \rangle_Y^2 \\ \langle \tilde{S}^{(3)}(\mathbf{x}, \mathbf{u}, \mathbf{v}) \rangle_Y &\simeq \langle S(\mathbf{x}, \mathbf{u}) \rangle_Y \langle S(\mathbf{u}, \mathbf{v}) \rangle_Y \langle S(\mathbf{v}, \mathbf{x}) \rangle_Y \\ \langle \tilde{S}^{(4)}(\mathbf{x}, \mathbf{y}, \mathbf{u}, \mathbf{v}) \rangle_Y &\simeq \langle Q(\mathbf{x}, \mathbf{y}, \mathbf{v}, \mathbf{u}) \rangle_Y \langle S(\mathbf{x}, \mathbf{u}) \rangle_Y \langle S(\mathbf{y}, \mathbf{v}) \rangle_Y. \end{aligned} \quad (2.26)$$

This immediately yields the large- N_c version of the squared amplitude in Eq. (2.19) :

$$\begin{aligned} \langle |\mathcal{M}(g(p)A \rightarrow g(k_1)g(k_2))|^2 \rangle_Y &= 16\bar{\alpha} (p^+)^2 z(1-z) P_{g \leftarrow g}(z) \\ &\times \int d^2\mathbf{x} d^2\mathbf{y} d^2\bar{\mathbf{x}} d^2\bar{\mathbf{y}} \frac{(\mathbf{x} - \mathbf{y}) \cdot (\bar{\mathbf{x}} - \bar{\mathbf{y}})}{(\mathbf{x} - \mathbf{y})^2 (\bar{\mathbf{x}} - \bar{\mathbf{y}})^2} e^{-i\mathbf{k}_1 \cdot (\mathbf{x} - \bar{\mathbf{x}}) - i\mathbf{k}_2 \cdot (\mathbf{y} - \bar{\mathbf{y}})} \\ &\times \left[\langle S(\mathbf{b}, \bar{\mathbf{b}}) \rangle_Y^2 - \langle S(\mathbf{b}, \bar{\mathbf{x}}) \rangle_Y \langle S(\bar{\mathbf{x}}, \bar{\mathbf{y}}) \rangle_Y \langle S(\bar{\mathbf{y}}, \mathbf{b}) \rangle_Y \right. \\ &\left. - \langle S(\bar{\mathbf{b}}, \mathbf{x}) \rangle_Y \langle S(\mathbf{x}, \mathbf{y}) \rangle_Y \langle S(\mathbf{y}, \bar{\mathbf{b}}) \rangle_Y + \langle Q(\mathbf{x}, \mathbf{y}, \bar{\mathbf{y}}, \bar{\mathbf{x}}) \rangle_Y \langle S(\mathbf{x}, \bar{\mathbf{x}}) \rangle_Y \langle S(\mathbf{y}, \bar{\mathbf{y}}) \rangle_Y \right], \end{aligned} \quad (2.27)$$

where $\bar{\alpha} \equiv \alpha_s N_c / \pi$ and the variables \mathbf{b} and $\bar{\mathbf{b}}$ have been defined after Eq. (2.19). As a check, one can easily verify that for a very asymmetric splitting ($z \ll 1$ or $1 - z \ll 1$), our Eq. (2.27) reduces, as it should, to the respective result in Refs. [13, 14].

(iii) Still at large N_c , the general Balitsky-JIMWLK hierarchy of coupled evolution equations for the multipole expectation values boils down to a triangular hierarchy of equations, which can be successively solved: the dipole S -matrix $\langle S \rangle_Y$ obeys a closed, non-linear equation, the BK equation [20, 51], while the quadrupole S -matrix $\langle Q \rangle_Y$ obeys an inhomogeneous equation which also involves $\langle S \rangle_Y$ (see e.g. [44]). This last equation is still quite complicated, but a good approximation to it — in the form of an analytic expression relating $\langle Q \rangle_Y$ to $\langle S \rangle_Y$ — can be obtained using a Gaussian approximation to the CGC weight function [13, 41–45].

To summarize, it is possible to explicitly evaluate Eq. (2.27), at least numerically, by combining a reasonable approximation for the dipole S -matrix — say, as given by the solution to the BK equation with a running coupling [66–69] — together with the expression for $\langle Q \rangle_Y$ valid in the Gaussian approximation and for large N_c (as given e.g. in Eq. (4.26) of Ref. [45]). This strategy has been recently applied to forward quark-gluon production ($qA \rightarrow qgX$) in Ref. [48], where the analog of Eq. (2.27) has been numerically computed and used for intensive studies of the di-hadron azimuthal correlations. (See also [16, 47, 70, 71] for related calculations.) We are confident that the corresponding study of Eq. (2.27) would pose no additional problems. In what follows, we shall consider specific kinematical limits in which our main results in this section, Eqs. (2.19) and (2.27), can be simplified via analytic approximations.

⁴Notice that, according to Eq. (2.23), the multipoles are normalized such that they remain of $\mathcal{O}(1)$ as $N_c \rightarrow \infty$.

3. Some special limits

In what follows we shall study some special kinematical limits of the result for two gluon production in Eq. (2.19). The first one refers to the case where the target nucleus is relatively dilute, or more precisely, when all the transverse momenta in the problem — meaning the transverse momenta $k_{1\perp}$ and $k_{2\perp}$ of the produced gluons *and* their momentum imbalance $K_\perp \equiv |\mathbf{k}_1 + \mathbf{k}_2|$ — are much larger than the target saturation momentum. In that case, one can study the interaction between the projectile partons and the target in the single-scattering approximation. In this limit, Eq. (2.19) will be shown to reduce to k_\perp -factorization on the target side, as expected. Then, in Sect. 3.2, we shall consider the more interesting case, also known as the “back-to-back correlation limit” [43], where the final transverse momenta are still very hard, $k_{1\perp}, k_{2\perp} \gg Q_s$, but their imbalance K_\perp is comparable to Q_s (its typical value in a collision). In that case, the effects of multiple scattering remain important, in that they determine the details of the angular distribution around its peak at $\Delta\Phi = \pi$. By performing appropriate approximations on Eq. (2.19), we shall make contact with the corresponding results in Ref. [43], that we shall extend to finite N_c . Finally, in Sect. 3.3, we shall discuss the “double parton scattering limit”, where the final gluons are produced by a nearly collinear splitting occurring long before the scattering. In that limit, our result (2.19) develops a logarithmic “infrared” divergence, which can be recognized as the contribution of two gluons from the projectile which independently scatter off the target. We shall explain how to cure this problem, thus following a procedure developed in Ref. [48] in the context of quark-gluon production.

3.1. The dilute target limit: angular correlations and k_\perp -factorization

Under the present assumptions, the total transverse momentum $\mathbf{K} \equiv \mathbf{k}_1 + \mathbf{k}_2$ of the two produced gluons is acquired exclusively via scattering off the nuclear target and hence it is of the order of $Q_s(A, Y)$ (the target saturation momentum at the relevant rapidity $Y = \ln(1/x_A)$). Indeed, $Q_s(A, Y)$ is the typical transverse momentum of the gluons from the nuclear wavefunction which participate in the scattering. Accordingly, if the final momenta \mathbf{k}_1 and \mathbf{k}_2 are much harder than Q_s , their imbalance $\mathbf{K} = \mathbf{k}_1 + \mathbf{k}_2$ in a typical event is relatively small, $K_\perp \sim Q_s \ll k_{1\perp}, k_{2\perp}$, meaning that the gluons propagate nearly back-to-back in the transverse plane. If the respective cross-section is plotted as a function of the azimuthal angle difference $\Delta\Phi = |\Phi_1 - \Phi_2|$ between the final gluons, it shows a peak at $\Delta\Phi = \pi$ with a small width $\delta\Phi \sim Q_s/\bar{k}_\perp$, where $\bar{k}_\perp = (k_{1\perp} + k_{2\perp})/2$. This situation can be studied within the single scattering (or dilute target) approximation, that is, by assuming that the total momentum \mathbf{K} is transferred via a single interaction, which involves either the original gluon from the projectile, or one of its two offsprings.

Strictly speaking, the dilute target approximation is justified provided \mathbf{K} itself is relatively hard, $K_\perp \gg Q_s$, since in that case the (unique) scattering probes the dilute part of the nuclear wavefunction well above saturation. But it remains marginally correct when K_\perp approaches Q_s from the above, in particular within the window for extended geometric scaling [54] where the target gluon distribution, although relatively dilute, is still influenced by saturation, via boundary effects at Q_s (see also [53, 55, 56]). This is the region that we shall study in this section. By evaluating Eq. (2.19) in the single scattering approximation, we will recover the usual form of k_\perp -factorization, in which the target is represented by the “unintegrated gluon distribution” obeying BFKL evolution [50]. Then, in the next subsection, we shall describe a more refined approximation scheme, introduced in Ref. [43], which allows one to properly treat the multiple scattering effects in the regime where $k_{1\perp}, k_{2\perp} \gg Q_s$, but $K_\perp \lesssim Q_s$.

The single scattering approximation amounts to evaluating the various colour multipoles which enter Eq. (2.19) for the squared amplitude in the 2-gluon exchange approximation. In turn this requires expanding the Wilson lines up to second order in the background field :

$$U(\mathbf{x}) = 1 + ig \int dx^+ \mathcal{A}^-(x^+, \mathbf{x}) - \frac{g^2}{2} \int dx^+ dy^+ \mathcal{P} \{ \mathcal{A}^-(x^+, \mathbf{x}) \mathcal{A}^-(y^+, \mathbf{x}) \} + \mathcal{O}(\mathcal{A}^3). \quad (3.1)$$

Then, clearly, the target expectation values involve only the 2-point function of \mathcal{A}^- , which is a measure of the gluon density in the nucleus. Gauge-invariance requires this 2-point function to be local in colour and in x^+ [65]. (We recall that the LC variable x^+ plays the role of time for the projectile and of the longitudinal coordinate for the target.) By also assuming the nucleus to be homogeneous in the transverse plane, for simplicity, we can write

$$\langle \mathcal{A}_a^-(x^+, \mathbf{x}) \mathcal{A}_b^-(y^+, \mathbf{y}) \rangle_Y = \delta^{ab} \delta(x^+ - y^+) \gamma_Y(x^+, \mathbf{x} - \mathbf{y}), \quad (3.2)$$

where the function $\gamma_Y(x^+, \mathbf{x} - \mathbf{y})$ depends upon the rapidity Y only via its support in x^+ . (With increasing Y , the longitudinal extent of the target increases via quantum evolution, i.e. via the inclusion of gluon modes with smaller and smaller values of x_A ; see e.g. [29, 45].) By inserting the expansion (3.1) into

the definitions (2.20) for the colour multipoles, keeping terms up to second order in the background field, and averaging over the latter according to Eq. (3.2), one finds

$$\begin{aligned}\langle \tilde{S}^{(2)}(\mathbf{x}, \mathbf{y}) \rangle_Y &= 1 - g^2 C_A \Gamma_Y(\mathbf{x} - \mathbf{y}) \\ \langle \tilde{S}^{(4)}(\mathbf{x}, \mathbf{y}, \mathbf{u}, \mathbf{v}) \rangle_Y &= 1 - \frac{g^2}{2} C_A \left[\Gamma_Y(\mathbf{x} - \mathbf{y}) - \Gamma_Y(\mathbf{x} - \mathbf{v}) - \Gamma_Y(\mathbf{y} - \mathbf{u}) \right. \\ &\quad \left. + \Gamma_Y(\mathbf{u} - \mathbf{v}) + 2\Gamma_Y(\mathbf{x} - \mathbf{u}) + 2\Gamma_Y(\mathbf{y} - \mathbf{v}) \right],\end{aligned}\quad (3.3)$$

where $C_A = N_c$ and $\Gamma_Y(\mathbf{r})$ stands for

$$\Gamma_Y(\mathbf{r}) \equiv \int dx^+ [\gamma_Y(x^+, \mathbf{0}) - \gamma_Y(x^+, \mathbf{r})]. \quad (3.4)$$

Within the present assumptions, the quantity $g^2 C_A \Gamma_Y(\mathbf{x} - \mathbf{y})$ is real and positive semi-definite and depends only upon $r_\perp = |\mathbf{x} - \mathbf{y}|$. It represents the dipole–nucleus scattering amplitude in the two–gluon exchange approximation for a gluonic dipole with transverse size r_\perp . (A similar expression with $C_A \rightarrow C_R$ holds for a dipole in an arbitrary representation R of the colour group.) For consistency with the present assumptions, this quantity must be computed by solving the linearized version of the BK equation, that is, the BFKL equation [17–19]. This equation strictly applies for sufficiently small dipoles with $r_\perp Q_s \ll 1$, but can be extended to the geometric scaling window if supplemented with an appropriate, “saturation”, boundary condition at $r_\perp \sim 1/Q_s$ [54, 55]

The single–scattering approximation to the squared amplitude (2.19) is then obtained as

$$\begin{aligned}\langle |\mathcal{M}(g(p)A \rightarrow g(k_1)g(k_2))|^2 \rangle_Y &= \frac{2g^4 N_c^2}{\pi^2} z(1-z) P_{g \leftarrow g}(z) \\ &\times \int d^2\mathbf{x} d^2\mathbf{y} d^2\bar{\mathbf{x}} d^2\bar{\mathbf{y}} \frac{(\mathbf{x} - \mathbf{y}) \cdot (\bar{\mathbf{x}} - \bar{\mathbf{y}})}{(\mathbf{x} - \mathbf{y})^2 (\bar{\mathbf{x}} - \bar{\mathbf{y}})^2} e^{-i\mathbf{k}_1 \cdot (\mathbf{x} - \bar{\mathbf{x}}) - i\mathbf{k}_2 \cdot (\mathbf{y} - \bar{\mathbf{y}})} \\ &\times \left[\Gamma_Y(\mathbf{b} - \bar{\mathbf{x}}) + \Gamma_Y(\mathbf{b} - \bar{\mathbf{y}}) + \Gamma_Y(\bar{\mathbf{b}} - \mathbf{x}) \right. \\ &\quad + \Gamma_Y(\bar{\mathbf{b}} - \mathbf{y}) + \Gamma_Y(\mathbf{x} - \bar{\mathbf{y}}) + \Gamma_Y(\mathbf{y} - \bar{\mathbf{x}}) + \\ &\quad \left. - 2\Gamma_Y(\mathbf{b} - \bar{\mathbf{b}}) - 2\Gamma_Y(\mathbf{x} - \bar{\mathbf{x}}) - 2\Gamma_Y(\mathbf{y} - \bar{\mathbf{y}}) \right].\end{aligned}\quad (3.5)$$

Remarkably, this result, which is valid for generic N_c , remains unchanged in the large- N_c limit.

It is now straightforward to perform the various Fourier transforms in Eq. (3.5). This procedure naturally introduces the following quantity⁵

$$f_Y(\mathbf{p}) \equiv -\mathbf{p}^2 \int d^2\mathbf{r} \Gamma_Y(\mathbf{r}) e^{-i\mathbf{p} \cdot \mathbf{r}} = \mathbf{p}^2 \int dx^+ \gamma_Y(x^+, \mathbf{p}), \quad (3.6)$$

generally referred to as the “unintegrated gluon distribution” (here, in the nucleus). For the dilute regime at hand, $f_Y(\mathbf{p})$ is the same as the *gluon occupation number*, that is, the number of gluons with $x = x_A$ and transverse momentum \mathbf{p} per unit rapidity and per unit transverse phase-space. The nucleus can be considered as ‘dilute’ so long as $f_Y(\mathbf{p}) \ll 1/\alpha$ [29], which is tantamount to the condition that the dipole amplitude be much smaller than one. Our normalization is such that the more conventional, ‘integrated’, gluon distribution, which enters the collinear factorization and counts the total number of gluons per unit rapidity as measured with a transverse resolution scale μ^2 , is obtained as (S_\perp denotes the transverse area of the nucleus)

$$x_A G_A(x_A; \mu^2) = \frac{S_\perp (N_c^2 - 1)}{4\pi^3} \int_{\mathbf{p}^2 < \mu^2} d^2\mathbf{p} f_Y(\mathbf{p}), \quad (3.7)$$

Returning to Eq. (3.5), one of the four transverse integrations there gives the transverse area S_\perp of the target, while the remaining three can be explicitly performed to yield

$$\begin{aligned}\langle |\mathcal{M}(g(p)A \rightarrow g(k_1)g(k_2))|^2 \rangle_Y &= 16g^4 N_c^2 S_\perp (p^+)^2 z(1-z) P_{g \leftarrow g}(z) \frac{f_Y(\mathbf{K})}{\mathbf{K}^2} \\ &\times \left[\frac{1}{\mathbf{P}^2} + \frac{1}{\mathbf{k}_1^2} + \frac{1}{\mathbf{k}_2^2} - \frac{\mathbf{P} \cdot \mathbf{k}_1}{\mathbf{P}^2 \mathbf{k}_1^2} + \frac{\mathbf{P} \cdot \mathbf{k}_2}{\mathbf{P}^2 \mathbf{k}_2^2} + \frac{\mathbf{k}_1 \cdot \mathbf{k}_2}{\mathbf{k}_1^2 \mathbf{k}_2^2} \right],\end{aligned}\quad (3.8)$$

⁵The sign in Eq. (3.6) is such as to ensure that $f_Y(\mathbf{p})$ is strictly positive with the present assumptions.

where $\mathbf{P} \equiv (1-z)\mathbf{k}_1 - z\mathbf{k}_2$ and we recall that $\mathbf{K} = \mathbf{k}_1 + \mathbf{k}_2$. For what follows, it is useful to keep in mind that \mathbf{K} and \mathbf{P} are the momenta conjugated to $\mathbf{b} = z\mathbf{x} + (1-z)\mathbf{y}$ and $\mathbf{r} = \mathbf{x} - \mathbf{y}$ (the center-of-mass and, respectively, the transverse separation of the two final gluons):

$$\mathbf{k}_1 \cdot \mathbf{x} + \mathbf{k}_2 \cdot \mathbf{y} = \mathbf{K} \cdot \mathbf{b} + \mathbf{P} \cdot \mathbf{r}. \quad (3.9)$$

Eq. (3.8) features the target occupation number $f_Y(\mathbf{K})$ for gluons with momentum $\mathbf{K} = \mathbf{k}_1 + \mathbf{k}_2$, as required by transverse momentum conservation. The function $f_Y(\mathbf{K})$ is roughly flat for $K_\perp \lesssim Q_s$ and it decreases quite fast when $K_\perp \gg Q_s$ (see below), hence the typical momentum transfers \mathbf{K} are such that $K_\perp \sim Q_s$, as anticipated. For such values, one has $P_\perp \simeq k_{1\perp} \simeq k_{2\perp} \gg K_\perp$ and Eq. (3.8) can be further simplified to (notice that $z(1-z)P_{g \leftarrow g}(z) = [1 - z(1-z)]^2$)

$$\frac{d\sigma(pA \rightarrow ggX)}{dy_1 dy_2 d^2\mathbf{k}_1 d^2\mathbf{k}_2} = x_p G(x_p, \mu^2) \frac{\bar{\alpha}^2}{\pi^2} [1 - z(1-z)]^3 S_\perp \frac{f_Y(\mathbf{k}_1 + \mathbf{k}_2)}{\mathbf{k}_1^4}. \quad (3.10)$$

This has been directly written for the respective cross-section, with the help of Eq. (2.5). Eq. (3.10) is the expected result in the single-scattering approximation. It features k_\perp -factorization at the level of the target side together with collinear factorization for the projectile. Both the target and the projectile are here assumed to be dilute, yet the respective degrees of diluteness are quite different — the intrinsic transverse momentum is negligible on projectile side, but not also on the target side —, which explains why Eq. (3.10) looks so asymmetric.

As already mentioned, Eq. (3.10) is strictly valid so long as $K_\perp \gg Q_s$ and marginally valid in the region of geometric scaling, whose extent is shown in Eq. (3.11) below. Within this region, one has [54, 55]

$$f_Y(\mathbf{p}) \sim \frac{1}{\bar{\alpha}} \left(\frac{Q_s^2(A, Y)}{p_\perp^2} \right)^{\gamma_s} \quad \text{for} \quad Q_s^2(A, Y) < p_\perp^2 < \frac{Q_s^4(A, Y)}{Q_0^2(A)}, \quad (3.11)$$

with $\gamma_s \simeq 0.63$ and $Q_0^2(A) = Q_s^2(A, Y_0)$ the nuclear saturation scale at the rapidity Y_0 at which one starts the high energy evolution (say, as given by the MV model [29]). Recalling that $Q_s^2(A, Y) \propto A^{1/3} e^{\lambda_s Y}$ with $\lambda_s \simeq 0.2 \div 0.3$ [68, 72], it is clear that the width of this region in p_\perp extends quite fast with increasing Y and/or A . Moreover, the geometric scaling property — the fact that the gluon occupation number depends upon the transverse momentum p_\perp , the target rapidity $Y = \ln(1/x_A)$ and the atomic number A only via the ratio $p_\perp/Q_s(A, Y)$ — holds also in the saturation regime at $p_\perp \lesssim Q_s$. The precise behavior of $f_Y(\mathbf{p})$ for $p_\perp \lesssim Q_s$ depends upon its actual definition: the extension of Eq. (3.6) in the non-linear regime at saturation is not unique (it depends upon the process at hand) and some examples will be given in the next section (see also [31, 32, 43]). But all such definitions have in common the fact that the growth of $f_Y(\mathbf{p})$ at small p_\perp is tamed by saturation [29, 32].

The above considerations together with Eq. (3.10) confirm that the typical momentum imbalance generated via scattering off the nuclear target is $|\mathbf{k}_1 + \mathbf{k}_2| \lesssim Q_s(A, Y)$ and also suggest that the azimuthal distribution should exhibit geometric scaling. Choosing for simplicity $k_{1\perp} = k_{2\perp} \equiv \bar{k}_\perp \gg Q_s$, such that $(\mathbf{k}_1 + \mathbf{k}_2)^2 = 2\bar{k}_\perp^2(1 + \cos \Delta\Phi) \simeq (\bar{k}_\perp \delta\Phi)^2$ (we set $\Delta\Phi = \pi - \delta\Phi$ with $\delta\Phi \ll 1$), we deduce that the cross-section (3.10) for two gluon production is peaked at $\delta\Phi \lesssim Q_s(A, Y)/\bar{k}_\perp$. Geometric scaling can then be viewed as follows: if one increases the rapidities y_1 and y_2 of the final gluons by the same amount Δy while simultaneously decreasing \bar{k}_\perp in such a way to keep constant values for x_p and z , then it is easily to check that the width $\delta\Phi$ of the angular distribution increases with Δy as $\delta\Phi \sim e^{(1+\lambda_s)\Delta y}$.

3.2. The back-to-back correlation limit

The previous discussion shows that, even for relatively hard final gluons with $k_{1\perp}, k_{2\perp} \gg Q_s$, the effects of multiple scattering remain important if one is interested in the details of the azimuthal distribution around its peak at $\Delta\Phi = \pi$. To study such effects, one needs to relax the single-scattering approximation in Sect. 3.1 while at the same time exploiting the hardness of the final momenta \mathbf{k}_1 and \mathbf{k}_2 . The proper strategy in that sense, as originally proposed in Ref. [43], relies on the observation that the relative momentum $\mathbf{P} = (1-z)\mathbf{k}_1 - z\mathbf{k}_2$ refers to the hard splitting which creates the gluon pair, while the total momentum \mathbf{K} accounts for the transverse momentum broadening of the two gluons via their (comparatively soft) interactions with the target. This is e.g. visible on Eq. (3.9), which shows that \mathbf{P} controls the transverse separation $\mathbf{r} = \mathbf{x} - \mathbf{y}$ between the offspring gluons in the direct amplitude (and similarly $\bar{\mathbf{r}} = \bar{\mathbf{x}} - \bar{\mathbf{y}}$ in the complex conjugate amplitude), whereas \mathbf{K} controls the difference $\mathbf{b} - \bar{\mathbf{b}}$ between the average positions of the gluons in the direct and the c.c. amplitude, which in turn encodes the effects of the multiple scattering with the target. Accordingly, in the interesting regime at $K_\perp \sim Q_s \ll P_\perp$ (a.k.a. the “back-to-back correlation limit”), the integral in (2.19) is controlled by configurations where

the transverse-size variables \mathbf{r} and $\bar{\mathbf{r}}$ are small compared to the difference $\mathbf{b} - \bar{\mathbf{b}}$ between the center-of-mass variables (and of course also small as compared to \mathbf{b} and $\bar{\mathbf{b}}$ themselves). This allows for appropriate Taylor expansions of the various S -matrices in Eq. (2.19).

Specifically, using the new variables $\mathbf{b}, \mathbf{r}, \bar{\mathbf{b}}, \bar{\mathbf{r}}$ and their conjugate momenta, Eq. (2.19) becomes :

$$\begin{aligned} \langle |\mathcal{M}(g(p)A \rightarrow g(k_1)g(k_2))|^2 \rangle_Y &= \frac{4g^2 N_c}{\pi^2} (p^+)^2 z(1-z) P_{g \leftarrow g}(z) \\ &\times \int d^2 \mathbf{b} d^2 \mathbf{r} d^2 \bar{\mathbf{b}} d^2 \bar{\mathbf{r}} \frac{\mathbf{r} \cdot \bar{\mathbf{r}}}{r^2 \bar{r}^2} e^{-i\mathbf{K} \cdot (\mathbf{b} - \bar{\mathbf{b}}) - i\mathbf{P} \cdot (\mathbf{r} - \bar{\mathbf{r}})} \\ &\times \left\langle \tilde{S}^{(2)}(\mathbf{b}, \bar{\mathbf{b}}) - \tilde{S}^{(3)}(\mathbf{b}, \bar{\mathbf{b}} + (1-z)\bar{\mathbf{r}}, \bar{\mathbf{b}} - z\bar{\mathbf{r}}) - \tilde{S}^{(3)}(\bar{\mathbf{b}}, \mathbf{b} + (1-z)\mathbf{r}, \mathbf{b} - z\mathbf{r}) \right. \\ &\quad \left. + \tilde{S}^{(4)}(\mathbf{b} + (1-z)\mathbf{r}, \mathbf{b} - z\mathbf{r}, \bar{\mathbf{b}} + (1-z)\bar{\mathbf{r}}, \bar{\mathbf{b}} - z\bar{\mathbf{r}}) \right\rangle_Y. \end{aligned} \quad (3.12)$$

We now expand the multipoles inside the integrand around \mathbf{b} and $\bar{\mathbf{b}}$. In view of the identities (2.21), it should be quite clear that the leading non trivial result arises from expanding $\tilde{S}^{(4)}$ up to second order in r^i and \bar{r}^i and keeping only the ‘off-diagonal’ terms which are bilinear in $r^i \bar{r}^j$. (The ‘diagonal’ terms proportional to either $r^i r^j$ or $\bar{r}^i \bar{r}^j$ cancel against similar terms arising from the expansion of the two pieces involving $\tilde{S}^{(3)}$, and the same happens for the terms which are linear in r^i or \bar{r}^i .) A straightforward calculation gives

$$\begin{aligned} &r^i \bar{r}^j [(1-z)\partial_x^i - z\partial_y^i] [(1-z)\partial_u^j - z\partial_v^j] \langle \tilde{S}^{(4)}(\mathbf{x}, \mathbf{y}, \mathbf{u}, \mathbf{v}) \rangle_Y \Big|_{\mathbf{b}\bar{\mathbf{b}}\bar{\mathbf{b}}\bar{\mathbf{b}}} \\ &= \frac{r^i \bar{r}^j}{N_c(N_c^2 - 1)} \text{Tr} \left\langle \left[(1-z)\partial^i \tilde{U}(\mathbf{b}) T^a \tilde{U}^\dagger(\mathbf{b}) - z\tilde{U}(\mathbf{b}) T^a \partial^i \tilde{U}^\dagger(\mathbf{b}) \right] \right. \\ &\quad \left. \times \left[(1-z)\tilde{U}(\bar{\mathbf{b}}) T^a \partial^j \tilde{U}^\dagger(\bar{\mathbf{b}}) - z\partial^j \tilde{U}(\bar{\mathbf{b}}) T^a \tilde{U}^\dagger(\bar{\mathbf{b}}) \right] \right\rangle_Y \\ &= \frac{r^i \bar{r}^j}{N_c(N_c^2 - 1)} \left[-2z(1-z) \text{Tr} \left\langle \partial^i \tilde{U}(\mathbf{b}) T^a \tilde{U}^\dagger(\mathbf{b}) \partial^j \tilde{U}(\bar{\mathbf{b}}) T^a \tilde{U}^\dagger(\bar{\mathbf{b}}) \right\rangle_Y \right. \\ &\quad \left. + [1 - 2z(1-z)] \text{Tr} \left\langle \partial^i \tilde{U}(\mathbf{b}) T^a \tilde{U}^\dagger(\mathbf{b}) \tilde{U}(\bar{\mathbf{b}}) T^a \partial^j \tilde{U}^\dagger(\bar{\mathbf{b}}) \right\rangle_Y \right], \end{aligned} \quad (3.13)$$

where the second equality is obtained after using the identity $\tilde{U} T^a \tilde{V}^\dagger = -(\tilde{V} T^a \tilde{U}^\dagger)^\top$, valid for colour matrices \tilde{U} and \tilde{V} in the adjoint representation. It is convenient to split the final expression in Eq. (3.13) into two pieces, one proportional to $z(1-z)$ and another one that is independent of z . The z -independent piece cannot be further simplified (it is proportional to a second derivative of $\tilde{S}^{(4)}$, as visible on the first line of (3.13)). The piece proportional to $z(1-z)$, on the other hand, can be written in a simpler form, namely as a second derivative of $\tilde{S}^{(2)}$, by using the same trick as the one used to get the last equality in (3.13). After also performing the integrals over \mathbf{r} and $\bar{\mathbf{r}}$ in Eq. (3.12), according to

$$\int d^2 \mathbf{r} d^2 \bar{\mathbf{r}} \frac{r^i r^k \bar{r}^j \bar{r}^l}{r^2 \bar{r}^2} e^{-i\mathbf{P} \cdot (\mathbf{r} - \bar{\mathbf{r}})} = \pi^2 \frac{\partial^2 \ln \mathbf{P}^2}{\partial P^i \partial P^k} \frac{\partial^2 \ln \mathbf{P}^2}{\partial P^j \partial P^l} = \frac{4\pi^2}{\mathbf{P}^4} \delta^{ij}, \quad (3.14)$$

one finally obtains

$$\begin{aligned} \langle |\mathcal{M}(g(p)A \rightarrow g(k_1)g(k_2))|^2 \rangle_Y &= 16g^2 N_c \frac{(p^+)^2 z(1-z)}{\mathbf{P}^4} P_{g \leftarrow g}(z) \\ &\times \int d^2 \mathbf{b} d^2 \bar{\mathbf{b}} e^{-i\mathbf{K} \cdot (\mathbf{b} - \bar{\mathbf{b}})} \left\langle \partial_x^i \partial_u^j \tilde{S}^{(4)}(\mathbf{x}, \mathbf{b}, \mathbf{u}, \bar{\mathbf{b}}) \Big|_{\mathbf{b}\bar{\mathbf{b}}\bar{\mathbf{b}}\bar{\mathbf{b}}} - z(1-z) \partial_b^i \partial_{\bar{b}}^j \tilde{S}^{(2)}(\mathbf{b}, \bar{\mathbf{b}}) \right\rangle_Y. \end{aligned} \quad (3.15)$$

Incidentally, Eq. (3.14) confirms that the transverse distances $|\mathbf{r}|$ and $|\bar{\mathbf{r}}|$ in both the direct and the complex conjugate amplitude are separately of order $1/P_\perp$, as anticipated.

Eq. (3.15) represents the full result (under the present assumptions) for the production of a pair of relatively hard gluons, with transverse momenta $k_{1\perp}, k_{2\perp} \gg Q_s(A, Y)$. This completes our previous result in Eq. (3.10) by including the non-linear effects accompanying the hard branching process, which describe the multiple scattering between the gluons involved in the branching and the nuclear target. As manifest on Eq. (3.15), these non-linear effects control the magnitude $K_\perp \equiv |\mathbf{k}_1 + \mathbf{k}_2|$ of the total transverse momentum of the pair: the target expectation values appearing in the integrand of Eq. (3.15) rapidly decay for transverse separations $|\mathbf{b} - \bar{\mathbf{b}}| \gg 1/Q_s$, which in turn implies that, typically, $K_\perp \lesssim Q_s$, in agreement with the (less rigorous) arguments in Sect. 3.1. The bi-local colour operators built with

the second derivatives of $\tilde{S}^{(4)}$ and $\tilde{S}^{(2)}$ which enter Eq. (3.15) can be viewed as generalizations of the unintegrated gluon distribution $f_Y(\mathbf{K})$ in Eq. (3.6) to the non linear regime. The one associated with $\tilde{S}^{(2)}$ (the ‘dipole gluon distribution’), namely

$$S_{\perp} f_Y^{\text{dip}}(\mathbf{K}) \equiv \frac{1}{g^2 N_c} \int d^2 \mathbf{b} d^2 \bar{\mathbf{b}} e^{-i \mathbf{K} \cdot (\mathbf{b} - \bar{\mathbf{b}})} \left\langle \partial_b^i \partial_{\bar{b}}^i \tilde{S}^{(2)}(\mathbf{b}, \bar{\mathbf{b}}) \right\rangle_Y, \quad (3.16)$$

is well-known known in the literature, as it enters various inclusive and semi-inclusive processes involving a dense target, like the total cross-section for deep inelastic scattering (DIS) and the single-inclusive parton production in DIS and p-A collisions (see Ref. [43] for a recent overview). The ‘quadrupole gluon distribution’ associated with $\tilde{S}^{(4)}$, that is,

$$S_{\perp} f_Y^{\text{quad}}(\mathbf{K}) \equiv \frac{1}{g^2 N_c} \int d^2 \mathbf{b} d^2 \bar{\mathbf{b}} e^{-i \mathbf{K} \cdot (\mathbf{b} - \bar{\mathbf{b}})} \left\langle \partial_x^i \partial_u^i \tilde{S}^{(4)}(\mathbf{x}, \mathbf{b}, \mathbf{u}, \bar{\mathbf{b}}) \right\rangle_{\mathbf{b} \bar{\mathbf{b}} \bar{\mathbf{b}}} \Big|_Y, \quad (3.17)$$

has not been introduced before to our knowledge, but its limit at large N_c has been studied in Ref. [43] (see also below). For the physical interpretation of these objects, $f_Y^{\text{dip}}(\mathbf{K})$ and $f_Y^{\text{quad}}(\mathbf{K})$, one should however keep in mind that they involve both ‘final-state’ and ‘initial-state’ interactions (that is, gluon-target interactions occurring both before and after the branching process), which cannot be simultaneously gauged away by a proper choice of the light-cone gauge for the target ($A^- = 0$). Hence, these quantities do not really measure the gluon occupation number⁶ except in the dilute target limit, where they both reduce to the standard gluon distribution (3.6), as one can easily check. (So, Eq. (3.15) properly reduces to Eq. (3.10) in that limit, as it should.)

The large- N_c limit of Eq. (3.15) is also interesting, in particular, because it allows us to make contact with the corresponding result in Ref. [43]. Namely, using the approximations (2.26) for the colour multipoles which appear in Eq. (3.15) one finds after some algebra

$$\begin{aligned} \left\langle |\mathcal{M}(g(p)A \rightarrow g(k_1)g(k_2))|^2 \right\rangle_Y &= 16g^2 N_c \frac{(p^+)^2 z(1-z)}{\mathbf{P}^4} P_{g \leftarrow g}(z) \int d^2 \mathbf{b} d^2 \bar{\mathbf{b}} e^{-i \mathbf{K} \cdot (\mathbf{b} - \bar{\mathbf{b}})} \\ &\times \left\{ [(1-z)^2 + z^2] \left\langle S(\mathbf{b}, \bar{\mathbf{b}}) \right\rangle_Y \partial_b^i \partial_{\bar{b}}^i \left\langle S(\mathbf{b}, \bar{\mathbf{b}}) \right\rangle_Y - 2z(1-z) \partial_b^i \left\langle S(\mathbf{b}, \bar{\mathbf{b}}) \right\rangle_Y \partial_{\bar{b}}^i \left\langle S(\mathbf{b}, \bar{\mathbf{b}}) \right\rangle_Y + \right. \\ &\left. + \left\langle S(\mathbf{b}, \bar{\mathbf{b}}) \right\rangle_Y^2 \partial_x^i \partial_u^i \left\langle Q(\mathbf{x}, \mathbf{b}, \bar{\mathbf{b}}, \mathbf{u}) \right\rangle_Y \Big|_{\mathbf{b}, \bar{\mathbf{b}}, \bar{\mathbf{b}}} \right\}, \end{aligned} \quad (3.18)$$

which is equivalent to Eq. (105) in Ref. [43], as one can easily check.

3.3. Double parton scattering limit

In the two previous subsections, we focused on the limit where the final gluons are produced by a hard process, so they emerge with relatively large transverse momenta, $k_{1\perp}, k_{2\perp} \gg Q_s(A, Y)$, which are strongly correlated: $k_{1\perp} \simeq k_{2\perp} \gg K_{\perp} \equiv |\mathbf{k}_1 + \mathbf{k}_2|$. In what follows, we shall rather study the opposite limit, in which the final transverse momenta are semi-hard, $k_{1\perp}, k_{2\perp} \lesssim Q_s$, and uncorrelated with each other — meaning that the two gluons scatter *independently* off the target. As discussed in Ref. [48], in the context of quark-gluon production ($qA \rightarrow qgX$), this situation occurs when the two final partons are produced by a nearly collinear splitting taking place in the remote past (long before the collision) and deserves special attention because it introduces an infrared divergence in the cross-section (see also below). In turn, this divergence can be associated with (one step in) the DGLAP evolution of the double-parton distribution in the projectile. Hence, it should be better viewed as a part of a different process, complementary to the one under consideration: the process in which two gluons preexisting in the proton wavefunction, as produced by the DGLAP evolution of the latter, independently scatter off the nuclear target. The probability to find such a gluon pair in the proton is expressed by the *double gluon distribution* $x_1 x_2 G^{(2)}(x_1, x_2, \mu^2)$, where the longitudinal momentum fractions x_1 and x_2 now refer to two independent partonic subprocesses, and read $x_1 = (k_{1\perp}/\sqrt{s}) e^{y_1}$ and $x_2 = (k_{2\perp}/\sqrt{s}) e^{y_2}$. The respective fractions for the gluons in the target are $x_{A1} = (k_{1\perp}/\sqrt{s}) e^{-y_1}$ and $x_{A1} = (k_{2\perp}/\sqrt{s}) e^{-y_2}$.

⁶Interestingly though, as pointed out in Ref. [43], the large- N_c decomposition of $f_Y^{\text{quad}}(\mathbf{K})$, cf. Eq. (2.26), involves a piece (the last piece in Eq. (3.18) below) which is proportional to the Weizsäcker-Williams gluon distribution and hence represents the gluon occupation number for a proper choice of the light-cone gauge.

The *double parton scattering* (DPS) contribution to the cross-section for two gluon production reads [48, 57]

$$\frac{d\sigma^{\text{DPS}}(pA \rightarrow ggX)}{dy_1 dy_2 d^2\mathbf{k}_1 d^2\mathbf{k}_2} = x_1 x_2 G^{(2)}(x_1, x_2, \mu^2) \frac{S_\perp}{(2\pi)^4} \langle \tilde{S}^{(2)}(\mathbf{k}_1) \rangle_Y \langle \tilde{S}^{(2)}(\mathbf{k}_2) \rangle_Y, \quad (3.19)$$

where $\langle \tilde{S}^{(2)}(\mathbf{k}) \rangle_Y$ denotes the Fourier transform of the gluonic dipole $\langle \tilde{S}^{(2)}(\mathbf{r}) \rangle_Y$ (which is the same as the ‘dipole gluon distribution’ in Eq. (3.16)), $Y = \ln(1/x_{A1}) \simeq \ln(1/x_{A2})$, and we recall that S_\perp denotes the transverse area of the nuclear target. As anticipated, Eq. (3.19) describe the independent scattering of the two gluons, hence it does not contribute to their azimuthal correlation, but only to the $\Delta\Phi$ -independent pedestal [57]. This DPS contribution must be added to that computed from Eq. (2.19) in order to obtain the total cross-section. To avoid double counting, one must however subtract the uncorrelated piece inherent in Eq. (2.19), which is also responsible for infrared divergences, as announced. This divergent piece will now be explicitly computed and shown to be indeed a particular contribution to Eq. (3.19). Our discussion below will be quite similar to that in Ref. [48], to which we refer for more details.

Specifically, the DPS-like contribution to Eq. (2.19) comes from the regime where the two gluons are widely separated in the transverse plane, meaning that both $\mathbf{r} = \mathbf{x} - \mathbf{y}$ (in the direct amplitude) and $\bar{\mathbf{r}} = \bar{\mathbf{x}} - \bar{\mathbf{y}}$ (in the complex conjugate amplitude) are much larger than the colour correlation length in the target $1/Q_s(A, Y)$. By contrast, the differences $|\mathbf{x} - \bar{\mathbf{x}}|$ and $|\mathbf{y} - \bar{\mathbf{y}}|$ are of order $1/Q_s$, hence they are comparatively small. Under these circumstances, the target colour fields at \mathbf{x} and \mathbf{y} (or $\bar{\mathbf{x}}$ and $\bar{\mathbf{y}}$) are independent from each other, hence they separately average out, and then the 4-point function $\langle \tilde{S}^{(4)} \rangle_Y$ factorizes into the product of two 2-point functions, one for each gluon:

$$\langle \tilde{S}^{(4)}(\mathbf{x}, \mathbf{y}, \bar{\mathbf{x}}, \bar{\mathbf{y}}) \rangle_Y \simeq \langle \tilde{S}^{(2)}(\mathbf{x}, \bar{\mathbf{x}}) \rangle_Y \langle \tilde{S}^{(2)}(\mathbf{y}, \bar{\mathbf{y}}) \rangle_Y. \quad (3.20)$$

The gluonic dipoles in the r.h.s. of Eq. (3.20) enforce $|\mathbf{x} - \bar{\mathbf{x}}|, |\mathbf{y} - \bar{\mathbf{y}}| \lesssim 1/Q_s$, as anticipated, but the transverse separations \mathbf{r} and $\bar{\mathbf{r}}$ are not constrained anymore. One of the corresponding integrations in Eq. (2.19) yields a factor S_\perp and the other one produces a logarithmic divergence (see below). For the same conditions, the 3-point functions like $\langle \tilde{S}^{(3)}(\mathbf{b}, \bar{\mathbf{x}}, \bar{\mathbf{y}}) \rangle_Y$ vanish: indeed, at least one of the three points \mathbf{b} , $\bar{\mathbf{x}}$, and $\bar{\mathbf{y}}$ is far away from the two others and the target expectation value of a single Wilson line vanishes by gauge symmetry. Finally, the 2-point function $\langle \tilde{S}^{(2)}(\mathbf{b}, \bar{\mathbf{b}}) \rangle_Y$ introduces no infrared divergence, since in the corresponding integrals in Eq. (2.19) the differences \mathbf{r} and $\bar{\mathbf{r}}$ are controlled by the external momenta, \mathbf{k}_1 and \mathbf{k}_2 , and hence cannot become arbitrarily large.

To summarize, infrared problems are generated only by the factorized piece (3.20) of $\langle \tilde{S}^{(4)} \rangle_Y$. This yields the following contribution to the squared amplitude (we recall that $\bar{\alpha} = \alpha_s N_c / \pi$):

$$\begin{aligned} \langle |\mathcal{M}(g(p)A \rightarrow g(k_1)g(k_2))|^2 \rangle_Y^{\text{DPS}} &= 16\bar{\alpha} S_\perp (p^+)^2 z(1-z) P_{g \leftarrow g}(z) \\ &\times \int \frac{d^2\mathbf{q}}{q^2} \langle \tilde{S}^{(2)}(\mathbf{k}_1 - \mathbf{q}) \rangle_Y \langle \tilde{S}^{(2)}(\mathbf{k}_2 + \mathbf{q}) \rangle_Y, \end{aligned} \quad (3.21)$$

which features two gluonic dipoles in the transverse-momentum representation. Note that the momentum variable \mathbf{q} is conjugate to the transverse separation \mathbf{r} (and also to $\bar{\mathbf{r}}$) between the produced gluons. The integral over \mathbf{q} is rapidly convergent in the ultraviolet ($q_\perp \rightarrow \infty$), by colour transparency, but it develops an infrared divergence in the collinear limit $q_\perp \rightarrow 0$, meaning for very large separations $r_\perp \rightarrow \infty$. Physically, we expect this divergence to be cured by confinement in the proton wavefunction. This whole physics — that of nearly collinear splittings and of their screening by confinement — is naturally included in the genuine DPS contribution, Eq. (3.19), which via the DGLAP evolution of the double-gluon distribution allows one to resum the large logarithms $\ln(\mu^2/\Lambda_{\text{QCD}}^2)$ to all orders. To avoid double counting, the DPS-like contributions must be subtracted from the matrix element squared (2.19). So long as the target saturation momentum $Q_s(A, Y)$ (which sets the scale for the external momenta $k_{1\perp}$ and $k_{2\perp}$) is much larger than the confinement scale Λ_{QCD} , this subtraction can be unambiguously performed, as we now explain.

To that aim, let us introduce an intermediate ‘factorization’ scale μ , such that $\Lambda_{\text{QCD}}^2 \ll \mu^2 \ll Q_s^2(A, Y)$. The contribution to Eq. (3.21) coming from the soft range at $\Lambda_{\text{QCD}} < q_\perp < \mu$ should be viewed as the ‘DPS-piece’ of our result (2.19) for the cross-section and subtracted from the latter. Within this piece, one can neglect q_\perp next to $k_{i\perp}$ and thus obtain

$$\begin{aligned} \left. \frac{d\sigma(pA \rightarrow ggX)}{dy_1 dy_2 d^2\mathbf{k}_1 d^2\mathbf{k}_2} \right|_{\text{DPS}} &= \bar{\alpha} x_p G(x_p, \mu^2) z(1-z) P_{g \leftarrow g}(z) \ln \frac{\mu^2}{\Lambda_{\text{QCD}}^2} \\ &\times \frac{S_\perp}{(2\pi)^4} \langle \tilde{S}^{(2)}(\mathbf{k}_1) \rangle_Y \langle \tilde{S}^{(2)}(\mathbf{k}_2) \rangle_Y, \end{aligned} \quad (3.22)$$

(This has been directly written as a contribution to the cross-section, with the help of Eq. (2.5).) Recalling that $x_p = x_1 + x_2$, $z = x_1/x_p$ and $1 - z = x_2/x_p$, it is clear that Eq. (3.22) is consistent with the genuine DPS cross-section in Eq. (3.19) provided one identifies

$$G^{(2)}(x_1, x_2, \mu^2) = \bar{\alpha} \frac{G(x_1 + x_2, \mu^2)}{x_1 + x_2} P_{g \leftarrow g} \left(\frac{x_1}{x_1 + x_2} \right) \ln \frac{\mu^2}{\Lambda_{\text{QCD}}^2}. \quad (3.23)$$

This identification is indeed correct: the r.h.s. of Eq. (3.23) is the expected result for the double-gluon distribution produced via one gluon decay ($g \rightarrow gg$) in one step of the DGLAP evolution (see e.g. [59]). Hence, by subtracting Eq. (3.22) from the cross-section built with the squared amplitude (2.19), we ensure that this particular contribution is included only once, as it should, via the DPS cross-section shown in Eq. (3.19).

Acknowledgements

We would like to thank Al Mueller for stimulating discussions and Fabio Dominguez, François Gelis, and Yacine Mehtar-Tani for helpful comments and for reading the manuscript. This work is supported by the Agence Nationale de la Recherche project # 11-BS04-015-01.

Appendix A. Background field propagator and Feynman rules

In this Appendix, we derive the Feynman rules that we use in Sect. 2.2 for computing gluon splitting in the presence of a shockwave. As explained in the main text, we work in the gauge $A^+ = 0$ to avoid the precession of the target colour current $J_a^\mu = \delta^{\mu-} J_a^-$ by the gluons radiated by the projectile. In this gauge, the target field has only a “minus” component: $\mathcal{A}_a^\mu = \delta^{\mu-} \mathcal{A}_a^-$. Then the total gauge field A_a^μ is the sum of this background field and the quantum fluctuations: $A_a^\mu = \delta^{\mu-} \mathcal{A}_a^- + a_a^\mu$, with $\mu = -, 1, 2$. The dynamics of the quantum gluons in the presence of the background field is described by the following action (see e.g. [73] for a derivation of this action in the light-cone gauge)

$$\begin{aligned} S_{\mathcal{A}}[\alpha] &\equiv S_{YM}[\mathcal{A} + a] - S_{YM}[\mathcal{A}] - \int d^4x \frac{\delta S_{YM}}{\delta A_a^\mu(x)} \Big|_{\mathcal{A}} a_a^\mu(x) \\ &= \frac{1}{2} \int d^4x d^4y a_a^\mu(x) (G^{-1})_{\mu\nu}^{ab}(x, y) a_b^\nu(y) + \int d^4x \mathcal{L}_{int}(x), \end{aligned} \quad (A.1)$$

where G^{-1} is the inverse of the background field propagator and \mathcal{L}_{int} contains the cubic and quartic interactions between the α fields in the presence of the target field.

Appendix A.1. Gluon propagator in a background field

We start by reviewing the construction of the background field propagator. This is defined as the solution to the following inhomogeneous equation

$$[\delta_\lambda^\mu \mathcal{D}_x^2 - \mathcal{D}_x^\mu \mathcal{D}_{x,\lambda} - 2ig\mathcal{F}_\lambda^\mu(x)]_{ac} G_{cb}^{\lambda\nu}(x, y) = i\delta^{ab} g^{\mu\nu} \delta^{(4)}(x - y), \quad (A.2)$$

where \mathcal{D} is the covariant derivative built with the background field and \mathcal{F} is the associated field strength tensor, which has only a single non-trivial component: $\mathcal{F}_a^{i-} = \partial^i \mathcal{A}_a^-$. Given the homogeneity of the background field in x^- , it is convenient to perform a Fourier transform to the k^+ -representation :

$$G_{ab}^{\mu\nu}(x, y) = \int \frac{dk^+}{2\pi} G_{ab}^{\mu\nu}(x^+, \mathbf{x}, y^+, \mathbf{y}; k^+) e^{-ik^+(x^- - y^-)}. \quad (A.3)$$

From now we use the notations $\vec{x} = (x^+, \mathbf{x})$ for the LC spatial components. Eq. (A.2) is easily shown to imply

$$\begin{aligned} G_{ab}^{-i}(\vec{x}, \vec{y}; k^+) &= \frac{i}{k^+} \partial_x^j G_{ab}^{ji}(\vec{x}, \vec{y}; k^+), & G_{ab}^{i-}(\vec{x}, \vec{y}; k^+) &= -\frac{i}{k^+} \partial_y^j G_{ab}^{ij}(\vec{x}, \vec{y}; k^+) \\ G_{ab}^{--}(\vec{x}, \vec{y}; k^+) &= \frac{i}{k^+} \partial_x^i G_{ab}^{i-}(\vec{x}, \vec{y}; k^+) = \frac{1}{(k^+)^2} \partial_x^i \partial_y^j G_{ab}^{ij}(\vec{x}, \vec{y}; k^+). \end{aligned} \quad (A.4)$$

All the components of the dressed propagator are written as differential operators acting on G^{ij} , to be determined.

By taking $(\mu, \nu) = (i, j)$ in (A.2) and using (A.4), we find

$$[-2ik^+ \mathcal{D}^- - \Delta_\perp]_{ac} G_{cb}^{ij}(\vec{x}, \vec{y}; k^+) = -i\delta^{ab}\delta^{ij}\delta^{(3)}(\vec{x} - \vec{y}), \quad (\text{A.5})$$

which up to a trivial δ^{ij} factor is recognized as the equation satisfied by the background field propagator of a massless *scalar* field: $G^{ij} = \delta^{ij}G$, with G the solution to

$$[-2ik^+(\partial^- - ig\mathcal{A}^-) - \Delta_\perp]_{ac} G^{cb}(\vec{x}, \vec{y}; k^+) = -i\delta^{ab}\delta^{(3)}(\vec{x} - \vec{y}). \quad (\text{A.6})$$

Ultimately, all the components of the gluon propagator are expressed in terms of this single scalar function:

$$\begin{aligned} G_{ab}^{ij}(\vec{x}, \vec{y}; k^+) &= \delta^{ij}G_{ab}(\vec{x}, \vec{y}; k^+) \\ G_{ab}^{-i}(\vec{x}, \vec{y}; k^+) &= \frac{i}{k^+} \partial_x^i G_{ab}(\vec{x}, \vec{y}; k^+) \\ G_{ab}^{i-}(\vec{x}, \vec{y}; k^+) &= -\frac{i}{k^+} \partial_y^i G_{ab}(\vec{x}, \vec{y}; k^+) \\ G_{ab}^{--}(\vec{x}, \vec{y}; k^+) &= \frac{1}{(k^+)^2} \partial_x^i \partial_y^i G_{ab}(\vec{x}, \vec{y}; k^+). \end{aligned} \quad (\text{A.7})$$

These relations can be summarized into the following shorthand notation :

$$G_{ab}^{\mu\nu}(\vec{x}, \vec{y}; k^+) = \mathcal{O}_{\vec{x}, \vec{y}, k^+}^{\mu\nu} G_{ab}(\vec{x}, \vec{y}; k^+); \quad (\text{A.8})$$

where $\mathcal{O}_{\vec{x}, \vec{y}, k^+}^{\mu\nu}$ is the differential operator :

$$\mathcal{O}_{\vec{x}, \vec{y}, k^+}^{\mu\nu} = \left(\delta^{\mu-} \frac{i}{k^+} \partial_x^i + \delta^{\mu i} \right) \left(-\delta^{\nu-} \frac{i}{k^+} \partial_y^i + \delta^{\nu i} \right). \quad (\text{A.9})$$

For the present purposes, one can assume that the shockwave is a δ -function in x^+ . In that case, the solution to Eq. (A.6) is well known and reads (see e.g. [25] for an explicit derivation)

$$\begin{aligned} G_{ab}(\vec{x}, \vec{y}; k^+) &= [\theta(x^+)\theta(y^+) + \theta(-x^+)\theta(-y^+)] \delta_{ab} G_0(\vec{x} - \vec{y}; k^+) \\ &\quad + 2k^+ \int_{z^+=0} d^2\mathbf{z} G_0(\vec{x} - \vec{z}; k^+) G_0(\vec{z} - \vec{y}; k^+) \\ &\quad [\theta(x^+)\theta(-y^+)\tilde{U}_{ab}(\mathbf{z}) - \theta(-x^+)\theta(y^+)\tilde{U}_{ab}^\dagger(\mathbf{z})] \end{aligned} \quad (\text{A.10})$$

where G_0 is the free scalar propagator (with the trivial colour structure δ^{ab} factorized out) and $\tilde{U}_{ab}(\mathbf{z})$ is the Wilson line in the adjoint representation, Eq. (2.2). The structure of Eq. (A.10) is easy to understand: either the two endpoints x and y lie on the same side of the shockwave, where the background field is zero along any causal propagation line matching x and y and thus the propagation is free, or they lie on the different sides of the shockwave, and then causality constrains the trajectory to cross the shockwave only once and thus acquire the colour precession represented by the Wilson line.

For deriving Feynman rules, it is convenient to represent the free scalar propagators within (A.10) in Fourier space. By also restoring the tensorial indices for the gluon propagator according to Eq. (A.8), one finds

$$G_{ab}^{\mu\nu}(\vec{x}, \vec{y}; k^+) = 2k^+ \int \frac{dp^- d^2\mathbf{p}}{(2\pi)^3} \frac{dq^- d^2\mathbf{q}}{(2\pi)^3} \frac{i\beta^{\mu i}(\mathbf{p}, k^+)}{p^2 + i\epsilon} \frac{i\beta^{\nu i}(\mathbf{q}, k^+)}{q^2 + i\epsilon} e^{-i\vec{p} \cdot \vec{x} + i\vec{q} \cdot \vec{y}} \int d^2\mathbf{z} \tilde{U}_{ab}(\mathbf{z}) e^{-i\mathbf{z} \cdot (\mathbf{p} - \mathbf{q})}, \quad (\text{A.11})$$

where $\vec{p} = (p^-, \mathbf{p})$ is the 3-momentum conjugate to \vec{x} and it is understood that $p^+ = q^+ = k^+$. In the second line, we have introduced the following decomposition for the Fourier space representation of the differential operator $\mathcal{O}_{\vec{x}, \vec{y}, k^+}^{\mu\nu}$:

$$\mathcal{O}_{\vec{p}, \vec{q}, k^+}^{\mu\nu} = \left(\delta^{\mu-} \frac{p^i}{k^+} + \delta^{\mu i} \right) \left(\delta^{\nu-} \frac{q^i}{k^+} + \delta^{\nu i} \right) \equiv \beta^{\mu i}(\mathbf{p}, k^+) \beta^{\nu i}(\mathbf{q}, k^+), \quad (\text{A.12})$$

with

$$\beta^{\mu i}(\mathbf{p}, k^+) = \delta^{\mu-} \frac{p^i}{k^+} + \delta^{\mu i}. \quad (\text{A.13})$$

The gauge condition $\epsilon^+ = 0$ together with the Ward identity $k \cdot \epsilon(k) = 0$ imply

$$\epsilon_\mu(k) \beta^{\mu i}(\mathbf{k}, k^+) = -\epsilon^i(k), \quad \beta^{\mu i}(\mathbf{k}, k^+) \epsilon^i(k) = \epsilon^\mu(k). \quad (\text{A.14})$$

These identities are useful in that they enable us to replace the polarization 4-vectors by their transverse components (the only ones to be independent).

Appendix A.2. Momentum space Feynman rules

Although we consider the scattering off an inhomogeneous background field (which has non-trivial dependences upon x^+ and \mathbf{x}), it is nevertheless convenient to use momentum-space Feynman rules. As usual, we shall denote the Lorentz piece of the 3-gluon vertex as

$$\Gamma_{\mu\nu\rho}(k, p, q) \equiv g_{\mu\nu}(k + p)_\rho + g_{\nu\rho}(q - p)_\mu - g_{\mu\rho}(k + q)_\nu. \quad (\text{A.15})$$

For convenience k has been chosen to be incoming and p and q outgoing. (We do not show the 4-gluon vertex, since this is not used in the present calculations.)

The only Feynman rules which are specific to the problem at hand refer to the gluon coupling to the shockwave. They will be detailed in what follows.

Appendix A.2.1. The gluon propagator in the shockwave

According to Eq. (A.11), the Feynman rule corresponding to Fig. A.2, that is, the propagator of a gluon which enters the shockwave with momentum q and which emerges with momentum p , reads

$$2k^+ \frac{i\beta^{\mu i}(\mathbf{p}, k^+)}{p^2 + i\epsilon} \frac{i\beta^{\nu i}(\mathbf{q}, k^+)}{q^2 + i\epsilon} \int d^2\mathbf{z} \tilde{U}_{ab}(\mathbf{z}) e^{-i\mathbf{z} \cdot (\mathbf{p} - \mathbf{q})}. \quad (\text{A.16})$$

The “plus” component of the momentum is not changed by the scattering off the shockwave: $p^+ = q^+ \equiv k^+$.

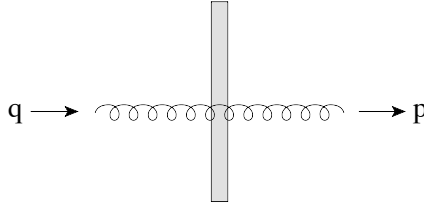


Figure A.2: Gluon coming into the shockwave with momentum q and emerging with momentum p .

Appendix A.2.2. External legs attached to the shockwave

An interesting, and rather subtle, question is: what is the rule corresponding to an external leg directly attached to the shockwave? Reduction formulæ generally instruct us to remove the external, free, propagators and replace them by polarization vectors, that is, either ϵ^μ or $\epsilon^{\mu*}$, depending on whether the gluons are in the initial state, or in the final state, respectively. This rule might suggest that, e.g., the initial gluon in the process shown on Fig. A.3 should bring a contribution

$$2k^+ \epsilon_\mu(k) \beta^{\mu i}(\mathbf{k}, k^+) \int_{p^+ \equiv k^+} \frac{dp^- d^2\mathbf{p}}{(2\pi)^3} \frac{i\beta^{\nu i}(\mathbf{p}, k^+)}{p^2 + i\epsilon} \int d^2\mathbf{z} \tilde{U}_{ab}(\mathbf{z}) e^{-i\mathbf{z} \cdot (\mathbf{p} - \mathbf{k})} M_\nu^b(p), \quad (\text{A.17})$$

where $M_\nu^b(p)$ is the Green function corresponding to the rest of the process represented by the bubble in Fig. A.3. Yet, this formula has a wrong sign as we shall shortly see.

To properly derive the Feynman rule corresponding to the process shown on Fig. A.3, according to the reduction formula, one needs to evaluate the following quantity

$$-i \int d^4x d^4y e^{-ikx} \epsilon^\mu(k) \square_x G_{\nu\mu}^{ba}(y, x) M^{b\nu}(y), \quad (\text{A.18})$$

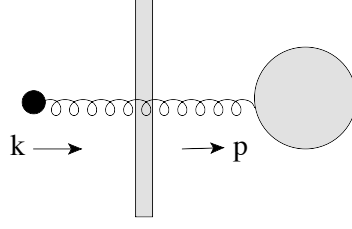


Figure A.3: Arbitrary process involving an initial gluon that crosses the shockwave.

where $M^{a\nu}(y)$ is the Fourier transform of $M^{a\nu}(k)$ with an incoming momentum k , that is⁷

$$M^{a\nu}(y) = \int \frac{d^4 k}{(2\pi)^4} M^{a\nu}(k) e^{iky}. \quad (\text{A.19})$$

Using (A.11), it is straightforward to rewrite the reduction formula (A.18) as

$$\begin{aligned} & -i \int d^4 x d^4 y e^{-ikx} \epsilon^\mu(k) \square_x G_{\nu\mu}^{ba}(y, x) M^{b\nu}(y) \\ & = -2k^+ \epsilon_\mu(k) \beta^{\mu i}(\mathbf{k}, k^+) \int_{p^+ \equiv k^+} \frac{dp^- d^2 \mathbf{p}}{(2\pi)^3} \frac{i\beta^{\nu i}(\mathbf{p}, k^+)}{p^2 + i\epsilon} \int d^2 \mathbf{z} \tilde{U}_{ba}(\mathbf{z}) e^{-i\mathbf{z}(\mathbf{p}-\mathbf{k})} M_\nu^b(p). \end{aligned} \quad (\text{A.20})$$

As anticipated, this formula differs from (A.17) by a sign.

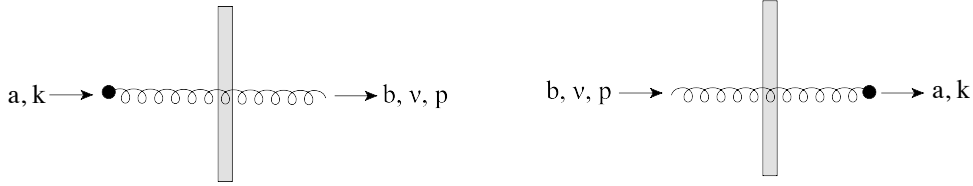


Figure A.4: Feynman diagrams corresponding respectively to the two formulæ in Eq. (A.21).

We now have the correct Feynman rules for external legs attached directly to the shockwave, which correspond respectively to the two figures represented on Fig. A.4 :

$$\begin{aligned} & -2k^+ \epsilon_\mu(k) \beta^{\mu i}(\mathbf{p}, k^+) \frac{i\beta^{\nu i}(\mathbf{p}, k^+)}{p^2 + i\epsilon} \int d^2 \mathbf{z} \tilde{U}_{ba}(\mathbf{z}) e^{-i\mathbf{z}(\mathbf{p}-\mathbf{k})}, \\ & -2k^+ \epsilon_\mu^*(k) \beta^{\mu i}(\mathbf{p}, k^+) \frac{i\beta^{\nu i}(\mathbf{p}, k^+)}{p^2 + i\epsilon} \int d^2 \mathbf{z} \tilde{U}_{ab}(\mathbf{z}) e^{-i\mathbf{r}(\mathbf{k}-\mathbf{p})}, \end{aligned} \quad (\text{A.21})$$

where it is understood that $p^+ = k^+$.

Appendix B. Some intermediate calculations

Here we detail some of the intermediate calculations leading to the results presented in Sect. 2.

⁷Please notice the unconventional sign in the exponential due to the fact that the momentum is *incoming*, rather than *outgoing*.

Appendix B.1. Computation of the squared vertices

In Sect. 2.3 one needs to compute three kinds of squared vertices which correspond to the sum over the polarizations of the square of (2.12). From the explicit form (A.13) of the $\beta^{\mu i}$'s one obtains

$$\begin{aligned}
& \beta^{\mu i}(\mathbf{k}_1 + \mathbf{k}_2, p^+) \beta^{\mu' i}(\mathbf{k}_1 + \mathbf{k}_2, p^+) \beta^{\nu j}(\mathbf{k}_1, k_1^+) \beta^{\nu' j}(\mathbf{k}_1, k_1^+) \beta^{\rho k}(\mathbf{k}_2, k_2^+) \beta^{\rho' k}(\mathbf{k}_2, k_2^+) \times \\
& \quad \times \Gamma_{\mu\nu\rho}(k_1 + k_2, k_1, k_2) \Gamma_{\mu'\nu'\rho'}(k_1 + k_2, k_1, k_2) = \frac{8((1-z)\mathbf{k}_1 - z\mathbf{k}_2)^2}{z(1-z)} P_{g \leftarrow g}(z). \\
& \beta^{\mu i}(\mathbf{k}_1 + \mathbf{k}_2, p^+) \beta^{\mu' i}(\mathbf{p}, p^+) \beta^{\nu j}(\mathbf{k}_1, k_1^+) \beta^{\nu' j}(\mathbf{l}, k_1^+) \beta^{\rho k}(\mathbf{k}_2, k_2^+) \beta^{\rho' k}(\mathbf{p} - \mathbf{l}, k_2^+) \times \\
& \quad \times \Gamma_{\mu\nu\rho}(k_1 + k_2, k_1, k_2) \Gamma_{\mu'\nu'\rho'}(p, l, p-l) = \frac{8\mathbf{l} \cdot ((1-z)\mathbf{k}_1 - z\mathbf{k}_2)}{z(1-z)} P_{g \leftarrow g}(z) \\
& \beta^{\mu i}(\mathbf{p}, p^+) \beta^{\mu' i}(\mathbf{p}, p^+) \beta^{\nu j}(\mathbf{l}, k_1^+) \beta^{\nu' j}(\mathbf{l}', k_1^+) \beta^{\rho k}(\mathbf{p} - \mathbf{l}, k_2^+) \beta^{\rho' k}(\mathbf{p} - \mathbf{l}', k_2^+) \times \\
& \quad \times \Gamma_{\mu\nu\rho}(p, l, p-l) \Gamma_{\mu'\nu'\rho'}(p, l', p-l') = \frac{8\mathbf{l} \cdot \mathbf{l}'}{z(1-z)} P_{g \leftarrow g}(z),
\end{aligned} \tag{B.1}$$

where $P_{g \leftarrow g}(z)$ is the DGLAP gluon to gluon splitting function (2.15). By using these results, one obtains the expression of the squared amplitude shown in Eq. (2.14).

Appendix B.2. Rewriting $\tilde{S}^{(4)}$ in terms of fundamental multipoles

In this Appendix, we shall demonstrate Eq. (2.22), that is, we shall rewrite the gluonic quadrupole operator $\tilde{S}^{(4)}$ introduced in (2.20) in term of colour multipoles made with Wilson lines in the fundamental representation. In this process, the following identities will be used:

$$\begin{aligned}
f^{abc} &= -2i \operatorname{tr}([t^a, t^b] t^c), \quad U t^a U^\dagger = t^b \tilde{U}_{ba} = (\tilde{U}^\dagger)_{ab} t^b \\
(t^a)_{ij} (t^a)_{kl} &= \frac{1}{2} \left(\delta_{il} \delta_{jk} - \frac{1}{N_c} \delta_{ij} \delta_{kl} \right)
\end{aligned} \tag{B.2}$$

Here, t^a denotes the $\text{SU}(N_c)$ generators in the fundamental representation, whereas U and respectively \tilde{U} refer to a same unitary matrix (e.g. a Wilson line) when this is written in the fundamental and, respectively, the adjoint representation of the colour group.

Starting with its definition (2.20), the function $\tilde{S}^{(4)}$ can be first rewritten by using the first two identities above:

$$\begin{aligned}
\tilde{S}^{(4)}(\mathbf{x}, \mathbf{y}, \mathbf{u}, \mathbf{v}) &= -\frac{4}{N_c(N_c^2 - 1)} \operatorname{tr} \{ [U^\dagger(\mathbf{x}) t^b U(\mathbf{x}), U^\dagger(\mathbf{y}) t^c U(\mathbf{y})] t^a \} \\
& \quad \times \operatorname{tr} \{ [U^\dagger(\mathbf{u}) t^b U(\mathbf{u}), U^\dagger(\mathbf{v}) t^c U(\mathbf{v})] t^a \}.
\end{aligned} \tag{B.3}$$

Next we successively get rid of all the t^a matrices by using the last identity in Eq. (B.2):

$$\begin{aligned}
\tilde{S}^{(4)}(\mathbf{x}, \mathbf{y}, \mathbf{u}, \mathbf{v}) &= \frac{2}{N_c(N_c^2 - 1)} \operatorname{tr} \{ [U^\dagger(\mathbf{x}) t^b U(\mathbf{x}), U^\dagger(\mathbf{y}) t^c U(\mathbf{y})] [U^\dagger(\mathbf{v}) t^c U(\mathbf{v}), U^\dagger(\mathbf{u}) t^b U(\mathbf{u})] \} \\
&= \dots \\
&= \frac{1}{2N_c(N_c^2 - 1)} \{ \operatorname{tr} [U(\mathbf{x}) U^\dagger(\mathbf{y}) U(\mathbf{v}) U^\dagger(\mathbf{u})] \operatorname{tr} [U(\mathbf{u}) U^\dagger(\mathbf{x})] \operatorname{tr} [U(\mathbf{y}) U^\dagger(\mathbf{v})] - \\
& \quad - \operatorname{tr} [U(\mathbf{x}) U^\dagger(\mathbf{y}) U(\mathbf{v}) U^\dagger(\mathbf{x}) U(\mathbf{u}) U^\dagger(\mathbf{v}) U(\mathbf{y}) U^\dagger(\mathbf{u})] + \text{h.c.} \}.
\end{aligned} \tag{B.4}$$

This last expression together with the definition (2.23) of the multipoles naturally leads to expression (2.22) for $\tilde{S}^{(4)}(\mathbf{x}, \mathbf{y}, \mathbf{u}, \mathbf{v})$.

References

- [1] **ALICE** Collaboration, B. Abelev *et al.*, “Pseudorapidity density of charged particles p-Pb collisions at $\sqrt{s_{NN}} = 5.02$ TeV,” [arXiv:1210.3615 \[nucl-ex\]](#).
- [2] **ALICE** Collaboration, B. Abelev *et al.*, “Transverse Momentum Distribution and Nuclear Modification Factor of Charged Particles in p-Pb Collisions at $\sqrt{s_{NN}} = 5.02$ TeV,” [arXiv:1210.4520 \[nucl-ex\]](#).

- [3] **CMS** Collaboration, S. Chatrchyan *et al.*, “Observation of long-range near-side angular correlations in proton-lead collisions at the LHC,” *Phys.Lett.* **B718** (2013) 795–814, [arXiv:1210.5482 \[nucl-ex\]](#).
- [4] **ALICE** Collaboration, B. Abelev *et al.*, “Long-range angular correlations on the near and away side in p -Pb collisions at $\sqrt{s_{NN}} = 5.02$ TeV,” *Phys.Lett.* **B719** (2013) 29–41, [arXiv:1212.2001 \[nucl-ex\]](#).
- [5] **ATLAS** Collaboration, G. Aad *et al.*, “Observation of Associated Near-side and Away-side Long-range Correlations in $\sqrt{s_{NN}} = 5.02$ TeV Proton-lead Collisions with the ATLAS Detector,” [arXiv:1212.5198 \[hep-ex\]](#).
- [6] **ATLAS** Collaboration, G. Aad *et al.*, “Measurement with the ATLAS detector of multi-particle azimuthal correlations in p +Pb collisions at $\sqrt{s_{NN}}=5.02$ TeV,” [arXiv:1303.2084 \[hep-ex\]](#).
- [7] **BRAHMS** Collaboration, I. Arsene *et al.*, “On the evolution of the nuclear modification factors with rapidity and centrality in $d + Au$ collisions at $s(NN)^{1/2} = 200$ -GeV,” *Phys.Rev.Lett.* **93** (2004) 242303, [arXiv:nucl-ex/0403005 \[nucl-ex\]](#).
- [8] **PHENIX** Collaboration, S. Adler *et al.*, “Nuclear modification factors for hadrons at forward and backward rapidities in deuteron-gold collisions at $s(NN)^{1/2} = 200$ -GeV,” *Phys.Rev.Lett.* **94** (2005) 082302, [arXiv:nucl-ex/0411054 \[nucl-ex\]](#).
- [9] **STAR** Collaboration, J. Adams *et al.*, “Forward neutral pion production in p + p and d + Au collisions at $s(NN)^{1/2} = 200$ -GeV,” *Phys.Rev.Lett.* **97** (2006) 152302, [arXiv:nucl-ex/0602011 \[nucl-ex\]](#).
- [10] E. Braidot, “Two-particle azimuthal correlations at forward rapidity in STAR,” [arXiv:1102.0931 \[nucl-ex\]](#).
- [11] **PHENIX** Collaboration, A. Adare *et al.*, “Suppression of back-to-back hadron pairs at forward rapidity in d + Au Collisions at $\sqrt{s_{NN}} = 200$ GeV,” *Phys.Rev.Lett.* **107** (2011) 172301, [arXiv:1105.5112 \[nucl-ex\]](#).
- [12] N. Nikolaev, W. Schafer, B. Zakharov, and V. Zoller, “Nonlinear k -perpendicular factorization for forward dijets in DIS off nuclei in the saturation regime,” *J.Exp.Theor.Phys.* **97** (2003) 441–465, [arXiv:hep-ph/0303024 \[hep-ph\]](#).
- [13] J. Jalilian-Marian and Y. V. Kovchegov, “Inclusive two-gluon and valence quark-gluon production in DIS and pA ,” *Phys.Rev.* **D70** (2004) 114017, [arXiv:hep-ph/0405266 \[hep-ph\]](#).
- [14] R. Baier, A. Kovner, M. Nardi, and U. A. Wiedemann, “Particle correlations in saturated QCD matter,” *Phys.Rev.* **D72** (2005) 094013, [arXiv:hep-ph/0506126 \[hep-ph\]](#).
- [15] C. Marquet, “Forward inclusive dijet production and azimuthal correlations in $p(A)$ collisions,” *Nucl.Phys.* **A796** (2007) 41–60, [arXiv:0708.0231 \[hep-ph\]](#).
- [16] J. L. Albacete and C. Marquet, “Azimuthal correlations of forward di-hadrons in d + Au collisions at RHIC in the Color Glass Condensate,” *Phys.Rev.Lett.* **105** (2010) 162301, [arXiv:1005.4065 \[hep-ph\]](#).
- [17] L. Lipatov, “Reggeization of the Vector Meson and the Vacuum Singularity in Nonabelian Gauge Theories,” *Sov.J.Nucl.Phys.* **23** (1976) 338–345.
- [18] E. Kuraev, L. Lipatov, and V. S. Fadin, “The Pomeranchuk Singularity in Nonabelian Gauge Theories,” *Sov.Phys.JETP* **45** (1977) 199–204.
- [19] I. Balitsky and L. Lipatov, “The Pomeranchuk Singularity in Quantum Chromodynamics,” *Sov.J.Nucl.Phys.* **28** (1978) 822–829.
- [20] I. Balitsky, “Operator expansion for high-energy scattering,” *Nucl.Phys.* **B463** (1996) 99–160, [arXiv:hep-ph/9509348 \[hep-ph\]](#).
- [21] Y. V. Kovchegov, “Small- x F2 structure function of a nucleus including multiple pomeron exchanges,” *Phys. Rev.* **D60** (1999) 034008, [arXiv:hep-ph/9901281](#).

- [22] J. Jalilian-Marian, A. Kovner, A. Leonidov, and H. Weigert, “The Wilson renormalization group for low x physics: Towards the high density regime,” *Phys.Rev.* **D59** (1998) 014014, [arXiv:hep-ph/9706377](#) [hep-ph].
- [23] J. Jalilian-Marian, A. Kovner, A. Leonidov, and H. Weigert, “The BFKL equation from the Wilson renormalization group,” *Nucl.Phys.* **B504** (1997) 415–431, [arXiv:hep-ph/9701284](#) [hep-ph].
- [24] J. Jalilian-Marian, A. Kovner, and H. Weigert, “The Wilson renormalization group for low x physics: Gluon evolution at finite parton density,” *Phys.Rev.* **D59** (1998) 014015, [arXiv:hep-ph/9709432](#) [hep-ph].
- [25] E. Iancu, A. Leonidov, and L. D. McLerran, “Nonlinear gluon evolution in the color glass condensate. 1.,” *Nucl.Phys.* **A692** (2001) 583–645, [arXiv:hep-ph/0011241](#) [hep-ph].
- [26] E. Iancu, A. Leonidov, and L. D. McLerran, “The Renormalization group equation for the color glass condensate,” *Phys.Lett.* **B510** (2001) 133–144, [arXiv:hep-ph/0102009](#) [hep-ph].
- [27] E. Ferreiro, E. Iancu, A. Leonidov, and L. McLerran, “Nonlinear gluon evolution in the color glass condensate. 2.,” *Nucl.Phys.* **A703** (2002) 489–538, [arXiv:hep-ph/0109115](#) [hep-ph].
- [28] **PHENIX Collaboration** Collaboration, S. Adler *et al.*, “Centrality dependence of π^0 and η production at large transverse momentum in $s(\text{NN})^{1/2} = 200\text{-GeV}$ d+Au collisions,” *Phys.Rev.Lett.* **98** (2007) 172302, [arXiv:nucl-ex/0610036](#) [nucl-ex].
- [29] E. Iancu and R. Venugopalan, “The color glass condensate and high energy scattering in QCD,” [arXiv:hep-ph/0303204](#).
- [30] H. Weigert, “Evolution at small $x(b_j)$: The color glass condensate,” *Prog. Part. Nucl. Phys.* **55** (2005) 461–565, [arXiv:hep-ph/0501087](#).
- [31] J. Jalilian-Marian and Y. V. Kovchegov, “Saturation physics and deuteron gold collisions at RHIC,” *Prog. Part. Nucl. Phys.* **56** (2006) 104–231, [arXiv:hep-ph/0505052](#).
- [32] F. Gelis, E. Iancu, J. Jalilian-Marian, and R. Venugopalan, “The Color Glass Condensate,” *Ann.Rev.Nucl.Part.Sci.* **60** (2010) 463–489, [arXiv:1002.0333](#) [hep-ph].
- [33] E. Iancu, “QCD in heavy ion collisions,” [arXiv:1205.0579](#) [hep-ph].
- [34] L. D. McLerran and R. Venugopalan, “Green’s functions in the color field of a large nucleus,” *Phys.Rev.* **D50** (1994) 2225–2233, [arXiv:hep-ph/9402335](#) [hep-ph].
- [35] J.-P. Blaizot, E. Iancu, and H. Weigert, “Non linear gluon evolution in path-integral form,” *Nucl. Phys.* **A713** (2003) 441–469, [arXiv:hep-ph/0206279](#).
- [36] K. Rummukainen and H. Weigert, “Universal features of JIMWLK and BK evolution at small x ,” *Nucl.Phys.* **A739** (2004) 183–226, [arXiv:hep-ph/0309306](#) [hep-ph].
- [37] T. Lappi, “Gluon spectrum in the glasma from JIMWLK evolution,” *Phys.Lett.* **B703** (2011) 325–330, [arXiv:1105.5511](#) [hep-ph].
- [38] A. Dumitru, J. Jalilian-Marian, T. Lappi, B. Schenke, and R. Venugopalan, “Renormalization group evolution of multi-gluon correlators in high energy QCD,” *Phys. Lett.* **B706** (2011) 219–224, [arXiv:1108.4764](#) [hep-ph].
- [39] E. Iancu, K. Itakura, and L. McLerran, “A Gaussian effective theory for gluon saturation,” *Nucl. Phys.* **A724** (2003) 181–222, [arXiv:hep-ph/0212123](#).
- [40] J. P. Blaizot, F. Gelis, and R. Venugopalan, “High energy p A collisions in the color glass condensate approach. II: Quark production,” *Nucl. Phys.* **A743** (2004) 57–91, [arXiv:hep-ph/0402257](#).
- [41] Y. V. Kovchegov, J. Kuokkanen, K. Rummukainen, and H. Weigert, “Subleading- $N(c)$ corrections in non-linear small- x evolution,” *Nucl.Phys.* **A823** (2009) 47–82, [arXiv:0812.3238](#) [hep-ph].
- [42] C. Marquet and H. Weigert, “New observables to test the Color Glass Condensate beyond the large- N_c limit,” *Nucl. Phys.* **A843** (2010) 68–97, [arXiv:1003.0813](#) [hep-ph].

- [43] F. Dominguez, C. Marquet, B.-W. Xiao, and F. Yuan, “Universality of Unintegrated Gluon Distributions at small x ,” *Phys.Rev.* **D83** (2011) 105005, [arXiv:1101.0715 \[hep-ph\]](#).
- [44] E. Iancu and D. Triantafyllopoulos, “Higher-point correlations from the JIMWLK evolution,” *JHEP* **1111** (2011) 105, [arXiv:1109.0302 \[hep-ph\]](#).
- [45] E. Iancu and D. Triantafyllopoulos, “JIMWLK evolution in the Gaussian approximation,” *JHEP* **1204** (2012) 025, [arXiv:1112.1104 \[hep-ph\]](#).
- [46] M. Alvioli, G. Soyez, and D. Triantafyllopoulos, “Testing the Gaussian Approximation to the JIMWLK Equation,” *Phys.Rev.* **D87** (2013) 014016, [arXiv:1212.1656 \[hep-ph\]](#).
- [47] A. Stasto, B.-W. Xiao, and F. Yuan, “Back-to-Back Correlations of Di-hadrons in dAu Collisions at RHIC,” *Phys.Lett.* **B716** (2012) 430–434, [arXiv:1109.1817 \[hep-ph\]](#).
- [48] T. Lappi and H. Mantysaari, “Forward dihadron correlations in deuteron-gold collisions with the Gaussian approximation of JIMWLK,” [arXiv:1209.2853 \[hep-ph\]](#).
- [49] F. Dominguez, C. Marquet, A. M. Stasto, and B.-W. Xiao, “Universality of multi-particle production in QCD at high energies,” *Phys.Rev.* **D87** (2013) 034007, [arXiv:1210.1141 \[hep-ph\]](#).
- [50] S. Catani, M. Ciaffaroni, and F. Hautmann, “The $k(t)$ factorization theorem for heavy flavor production at high-energy,” *Nucl.Phys.Proc.Suppl.* **23B** (1991) 328–335.
- [51] Y. V. Kovchegov and A. H. Mueller, “Gluon production in current nucleus and nucleon - nucleus collisions in a quasiclassical approximation,” *Nucl.Phys.* **B529** (1998) 451–479, [arXiv:hep-ph/9802440 \[hep-ph\]](#).
- [52] Y. V. Kovchegov and K. Tuchin, “Inclusive gluon production in DIS at high parton density,” *Phys. Rev.* **D65** (2002) 074026, [arXiv:hep-ph/0111362](#).
- [53] A. M. Stasto, K. J. Golec-Biernat, and J. Kwiecinski, “Geometric scaling for the total gamma* p cross-section in the low x region,” *Phys. Rev. Lett.* **86** (2001) 596–599, [arXiv:hep-ph/0007192](#).
- [54] E. Iancu, K. Itakura, and L. McLerran, “Geometric scaling above the saturation scale,” *Nucl. Phys.* **A708** (2002) 327–352, [arXiv:hep-ph/0203137](#).
- [55] A. H. Mueller and D. N. Triantafyllopoulos, “The energy dependence of the saturation momentum,” *Nucl. Phys.* **B640** (2002) 331–350, [arXiv:hep-ph/0205167](#).
- [56] S. Munier and R. B. Peschanski, “Geometric scaling as traveling waves,” *Phys. Rev. Lett.* **91** (2003) 232001, [arXiv:hep-ph/0309177](#).
- [57] M. Strikman and W. Vogelsang, “Multiple parton interactions and forward double pion production in pp and dA scattering,” *Phys.Rev.* **D83** (2011) 034029, [arXiv:1009.6123 \[hep-ph\]](#).
- [58] V.N. Gribov and L.N. Lipatov, *Sov. Journ. Nucl. Phys.* **15** (1972), 438; G. Altarelli and G. Parisi, *Nucl. Phys.* **B126** (1977), 298; Yu. L. Dokshitzer, *Sov. Phys. JETP* **46** (1977), 641.
- [59] J. R. Gaunt and W. J. Stirling, “Double Parton Distributions Incorporating Perturbative QCD Evolution and Momentum and Quark Number Sum Rules,” *JHEP* **1003** (2010) 005, [arXiv:0910.4347 \[hep-ph\]](#).
- [60] F. Gelis and Y. Mehtar-Tani, “Gluon propagation inside a high-energy nucleus,” *Phys.Rev.* **D73** (2006) 034019, [arXiv:hep-ph/0512079 \[hep-ph\]](#).
- [61] **HERA Combined Structure Functions Working Group** Collaboration, C. Gwenlan, “Combined HERA Deep Inelastic Scattering Data and NLO QCD Fits,” *Nucl.Phys.Proc.Suppl.* **191** (2009) 5–15, [arXiv:0902.1807 \[hep-ex\]](#).
- [62] “Proceedings of saturation, the Color Glass Condensate and the Glasma: What Have We Learned from RHIC?,” *Nucl. Phys. A* **854** (2011) 1–256.
- [63] F. Gelis and J. Jalilian-Marian, “Photon production in high-energy proton nucleus collisions,” *Phys.Rev.* **D66** (2002) 014021, [arXiv:hep-ph/0205037 \[hep-ph\]](#).

- [64] Y. V. Kovchegov, L. Szymanowski, and S. Wallon, “Perturbative odderon in the dipole model,” *Phys.Lett.* **B586** (2004) 267–281, [arXiv:hep-ph/0309281](#) [hep-ph].
- [65] Y. Hatta, E. Iancu, K. Itakura, and L. McLerran, “Odderon in the color glass condensate,” *Nucl.Phys.* **A760** (2005) 172–207, [arXiv:hep-ph/0501171](#) [hep-ph].
- [66] I. Balitsky, “Quark contribution to the small-x evolution of color dipole,” *Phys.Rev.* **D75** (2007) 014001, [arXiv:hep-ph/0609105](#) [hep-ph].
- [67] Y. V. Kovchegov and H. Weigert, “Triumvirate of Running Couplings in Small-x Evolution,” *Nucl.Phys.* **A784** (2007) 188–226, [arXiv:hep-ph/0609090](#) [hep-ph].
- [68] J. L. Albacete and Y. V. Kovchegov, “Solving high energy evolution equation including running coupling corrections,” *Phys.Rev.* **D75** (2007) 125021, [arXiv:0704.0612](#) [hep-ph].
- [69] I. Balitsky and G. A. Chirilli, “Next-to-leading order evolution of color dipoles,” *Phys.Rev.* **D77** (2008) 014019, [arXiv:0710.4330](#) [hep-ph].
- [70] J. L. Albacete and C. Marquet, “Single Inclusive Hadron Production at RHIC and the LHC from the Color Glass Condensate,” *Phys.Lett.* **B687** (2010) 174–179, [arXiv:arXiv:1001.1378](#) [hep-ph].
- [71] J. Kuokkanen, K. Rummukainen, and H. Weigert, “HERA-Data in the Light of Small x Evolution with State of the Art NLO Input,” *Nucl.Phys.* **A875** (2012) 29–93, [arXiv:1108.1867](#) [hep-ph].
- [72] D. N. Triantafyllopoulos, “The energy dependence of the saturation momentum from RG improved BFKL evolution,” *Nucl. Phys.* **B648** (2003) 293–316, [arXiv:hep-ph/0209121](#).
- [73] I. Balitsky, “Factorization and high-energy effective action,” *Phys.Rev.* **D60** (1999) 014020, [arXiv:hep-ph/9812311](#) [hep-ph].